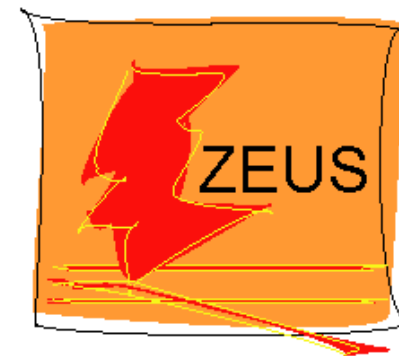


Jets at HERA: New look using NNLO

Radek Žlebčík¹

¹ Deutsches Elektronen-Synchrotron (DESY)

BNL, July 23



DESY-17-137 Eur.Phys.J.C77 (2017), 791 [arxiv:1709.07251]

DESY-18-054 Eur.Phys.J.C78 (2018), 538 [arxiv:1804.05663]

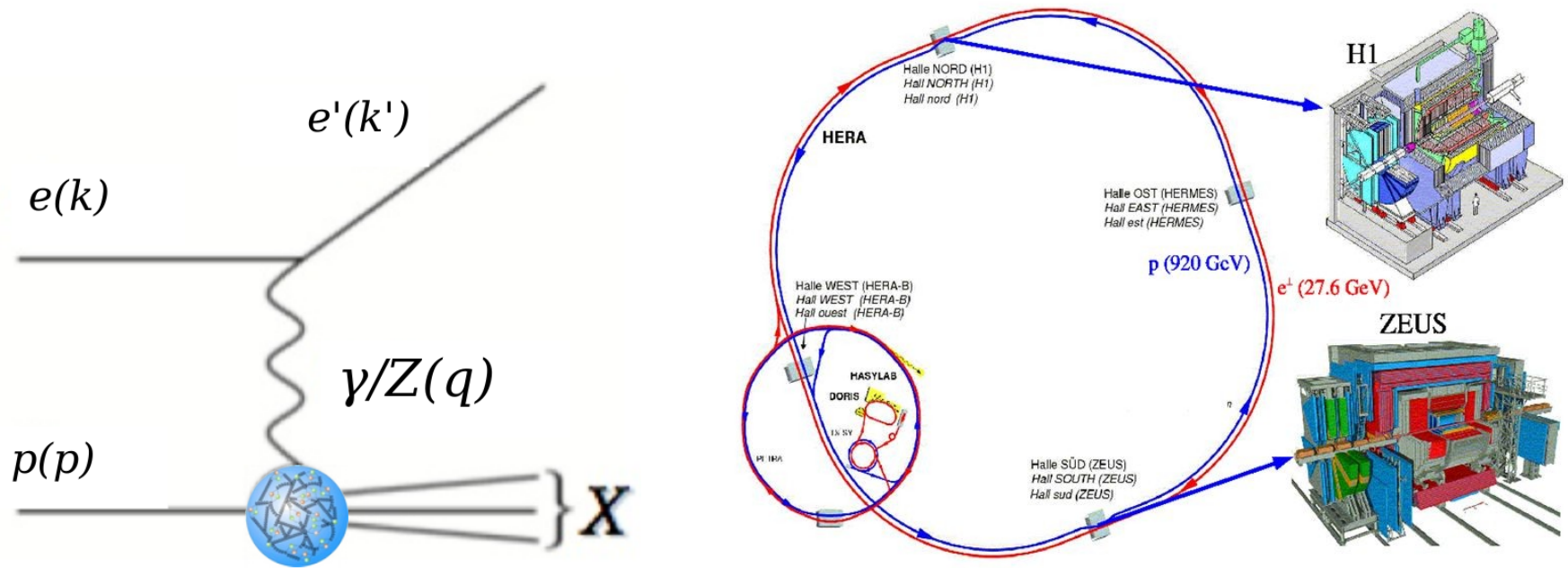
HERA Collider

- The only existing ep collider (1992 - 2007)
- About **0.5 fb⁻¹** of data per experiment
- Two multi-purpose detectors (**H1** + **ZEUS**)

$$e^{\pm} + p$$

$$27.6 \text{ GeV} + 920 \text{ GeV}$$

$$\sqrt{s} = 319 \text{ GeV}$$

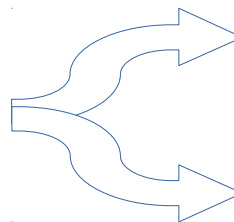


Inelasticity

$$y = \frac{p \cdot q}{p \cdot k}$$

Photon virtuality

$$Q^2 = -(k - k')^2$$



$$Q^2 \approx 0$$

Photoproduction

$$Q^2 \gg 0$$

Deep-inelastic scattering (DIS)

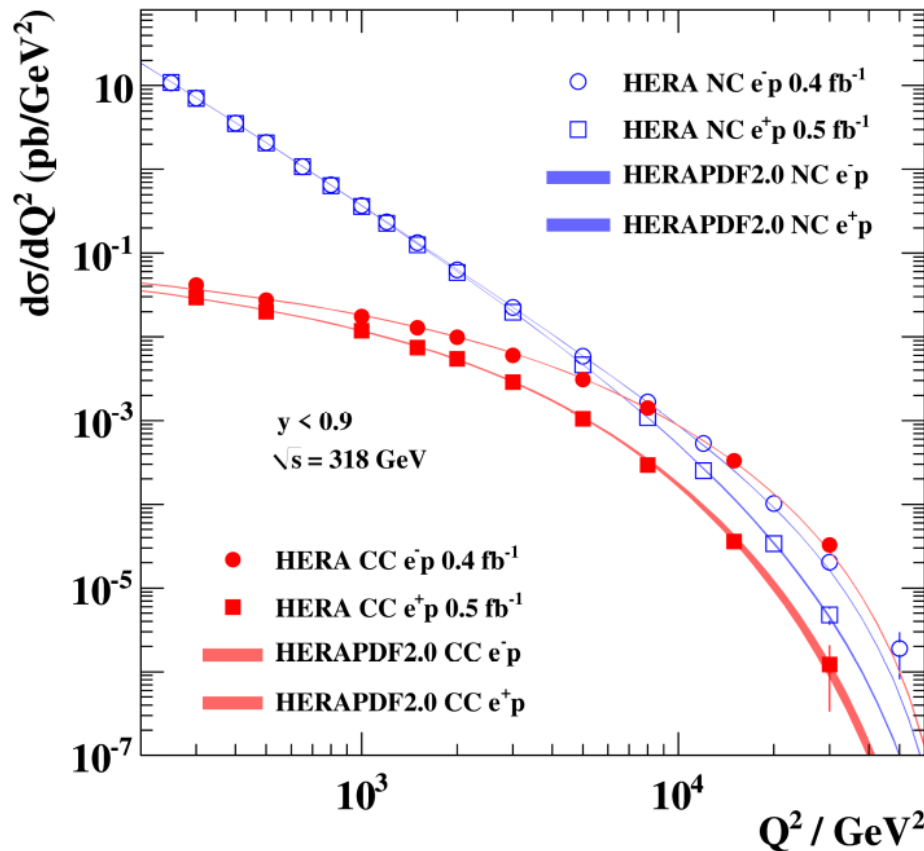
HERA Legacy

- Combined HERA NC+CC inclusive reduced cross sections (0.5 fb^{-1} per experiment)

[arxiv:1506.06042]

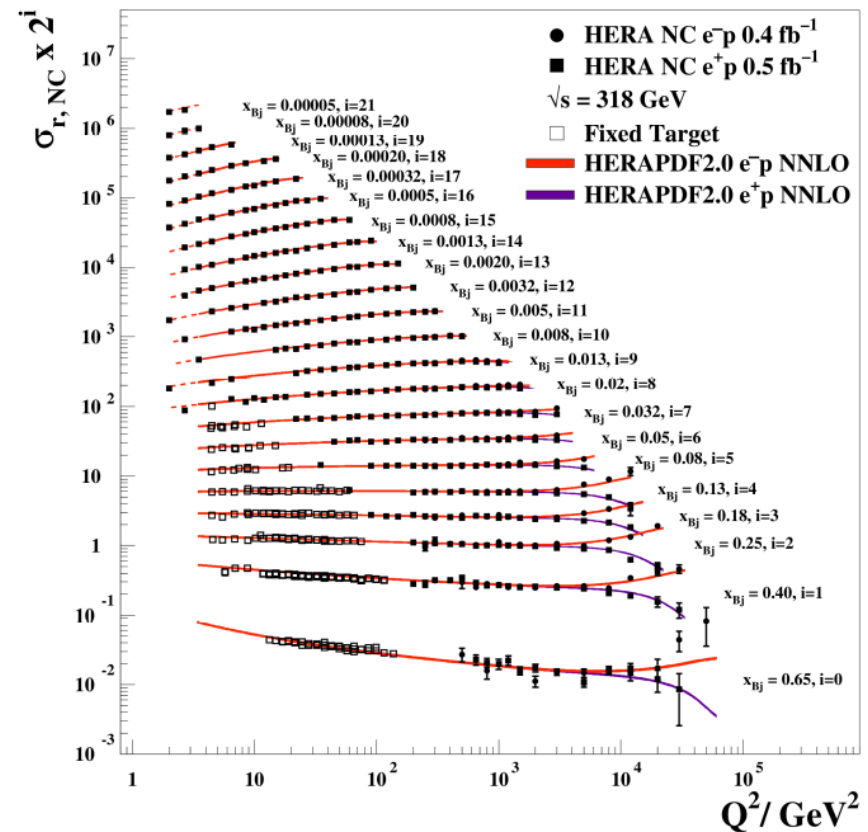
EW Unification

H1 and ZEUS



Bjorken Scaling

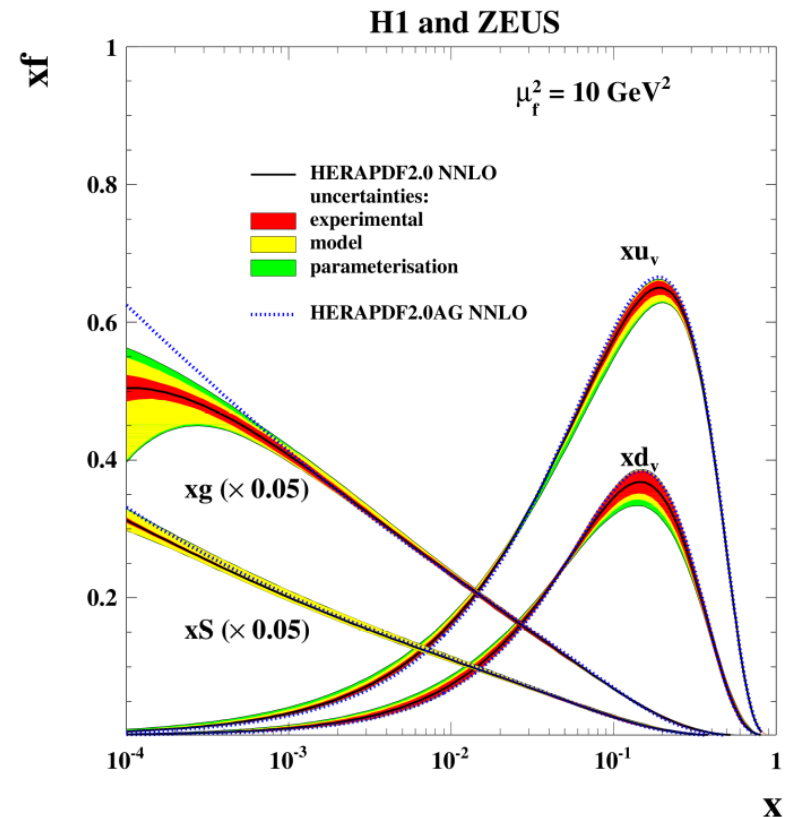
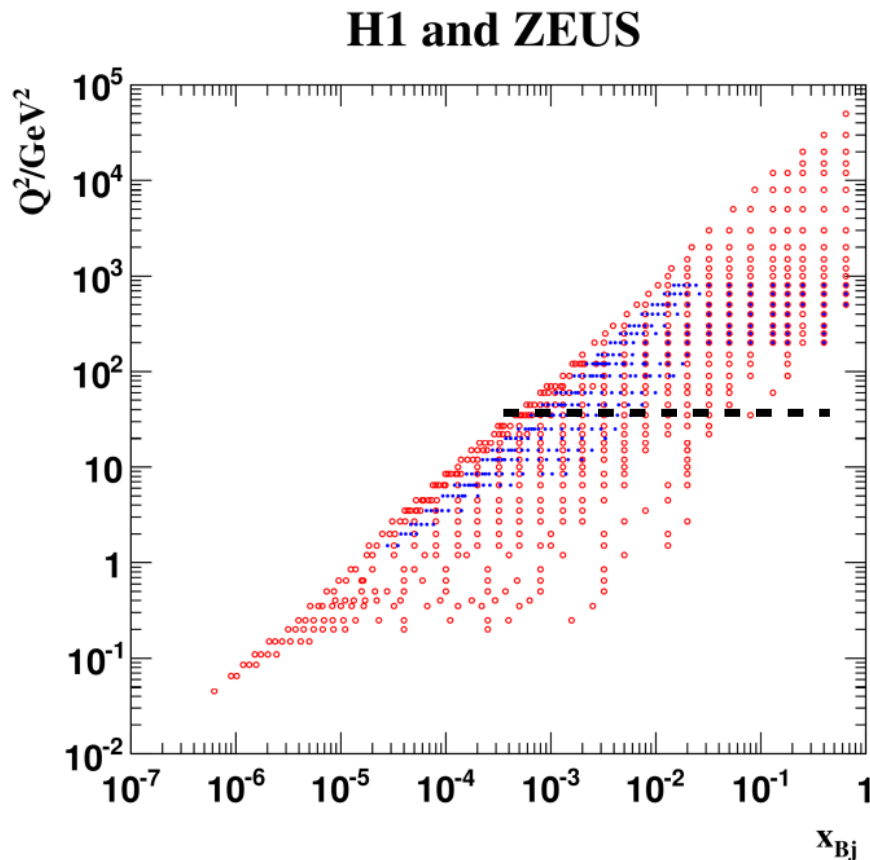
H1 and ZEUS



HERA Legacy

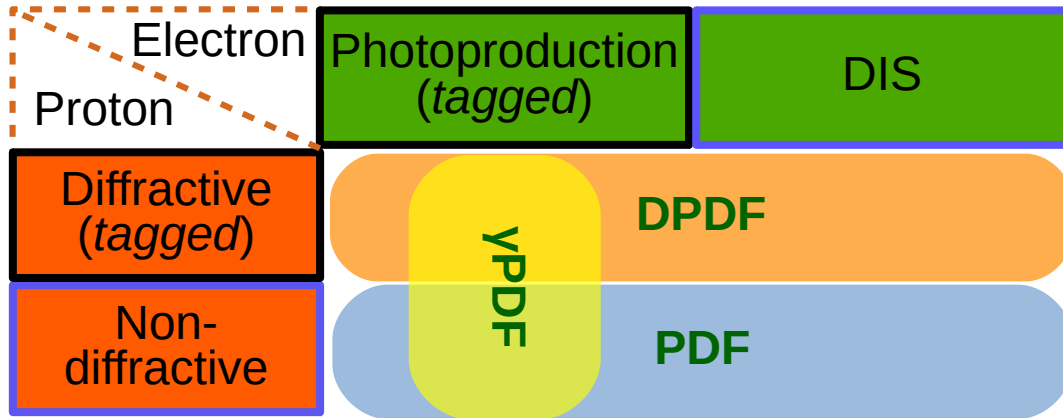
[arxiv:1506.06042]

- Large coverage in x , Q^2
limitation due to beam energy and acceptance
- HERAPDF2.0 QCD fit
based exclusively on
HERA inclusive DIS data

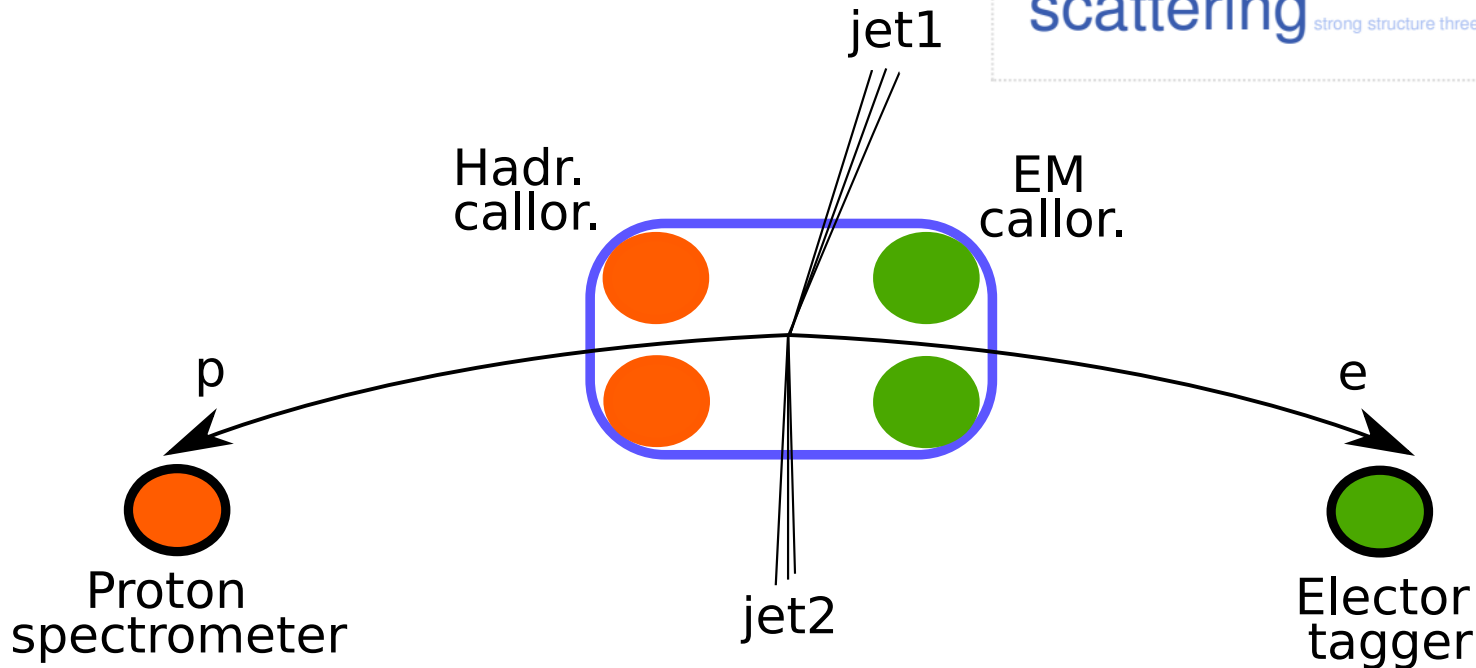


Jet production at HERA

- Basic classification according the state of proton and electron after scattering

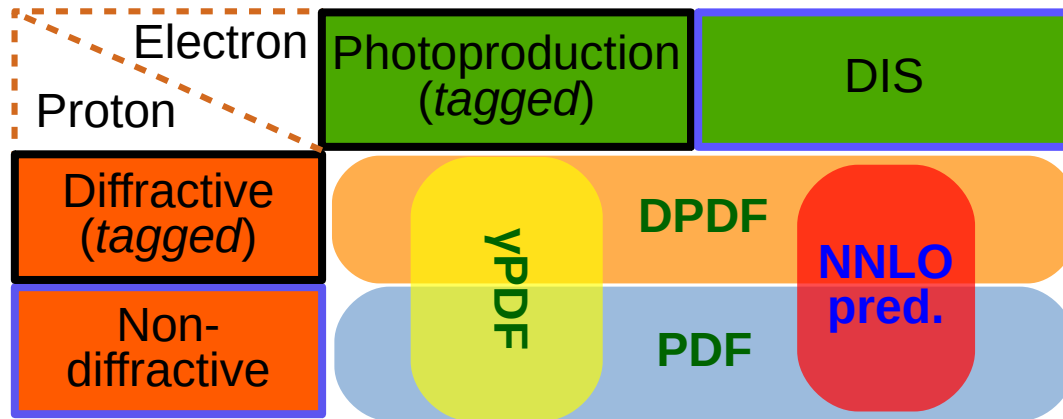


In total 118 Jet analyses from HERA

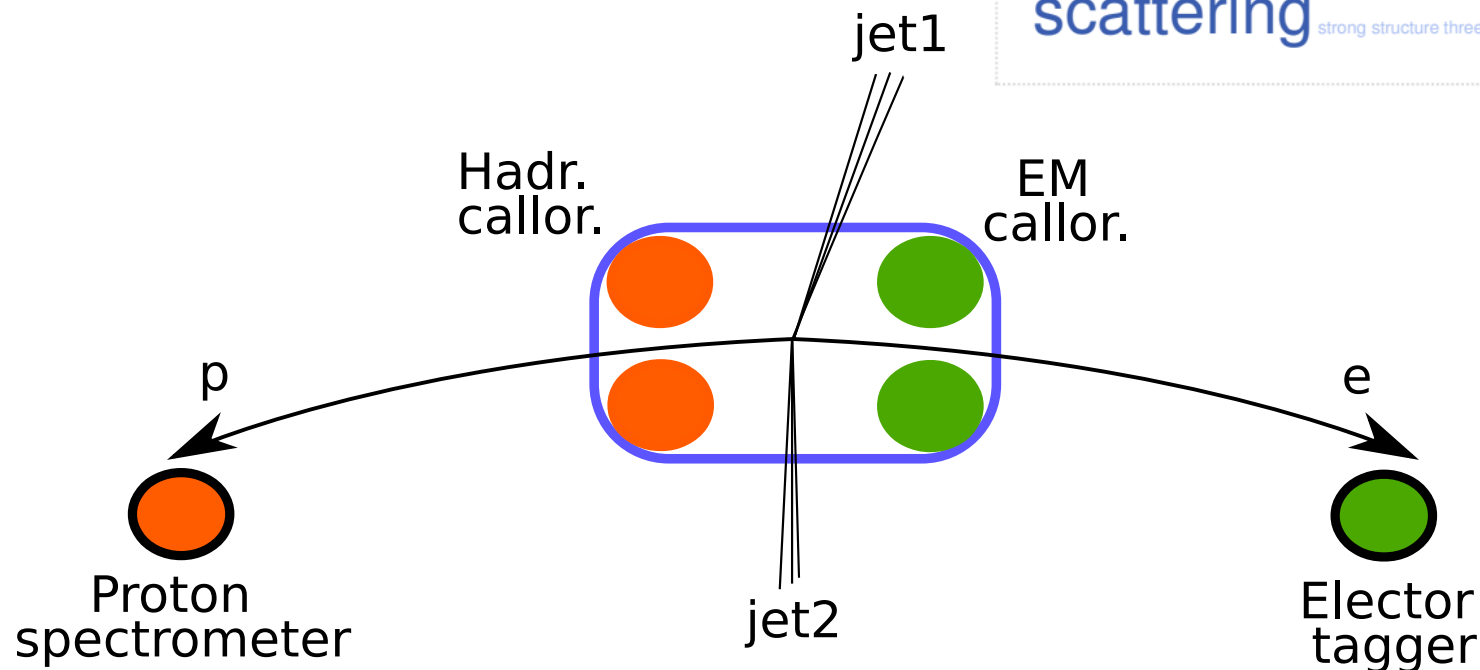


Jet production at HERA

- Basic classification according the state of proton and electron after scattering



In total 118 Jet analyses from HERA



NNLO calculations

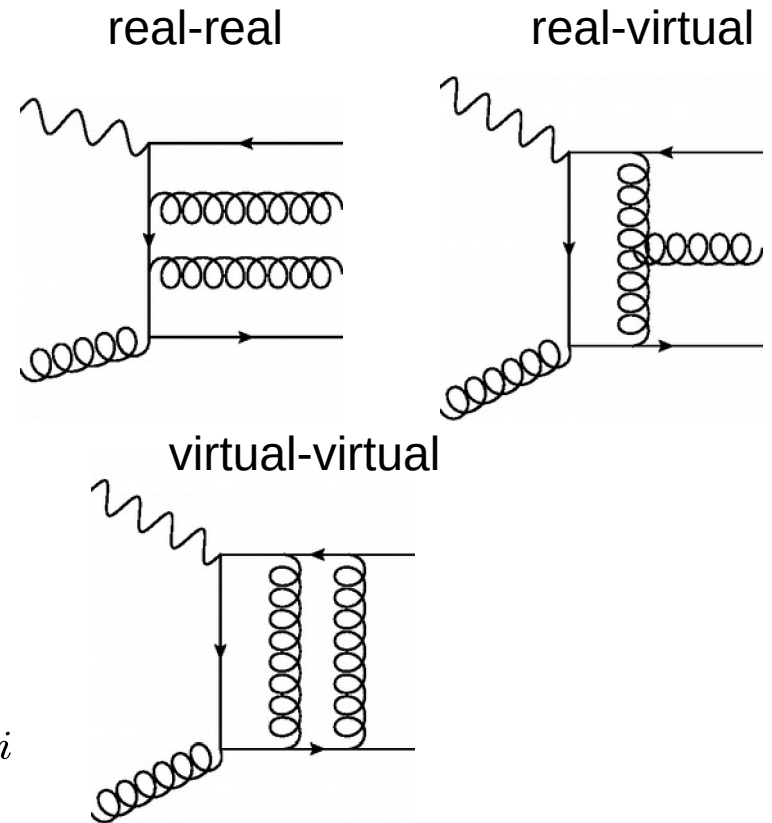
✓ Real-real + real-virtual crosschecked with NLOJET++ & SHERPA

- New NNLO predictions for ep dijets based on **antenna subtraction**
J. Currie, T. Gehrmann, A. Huss and J. Niehues, JHEP 07 (2017) 018, [1703.05977]
- **Matrix element** tables precalculated by **NNLOJET** program (~100 CPU years)
- Then convoluted with PDFs and α_S with **fastNLO** using the **APPLfast** interface (<1s)

$$\sigma_i = \sum_{k=g,q,\bar{g}} \int dx f_k(x, \mu_F) \hat{\sigma}_{i,k}(x, \mu_R, \mu_F) \cdot c_{\text{had},i}$$

$$\hat{\sigma}_{i,k}(x, \mu_R, \mu_F) =$$

$$\sum_n \alpha_S^n(\mu_R) \hat{\sigma}_{i,k}^{(n)}(x, \mu_R, \mu_F)$$

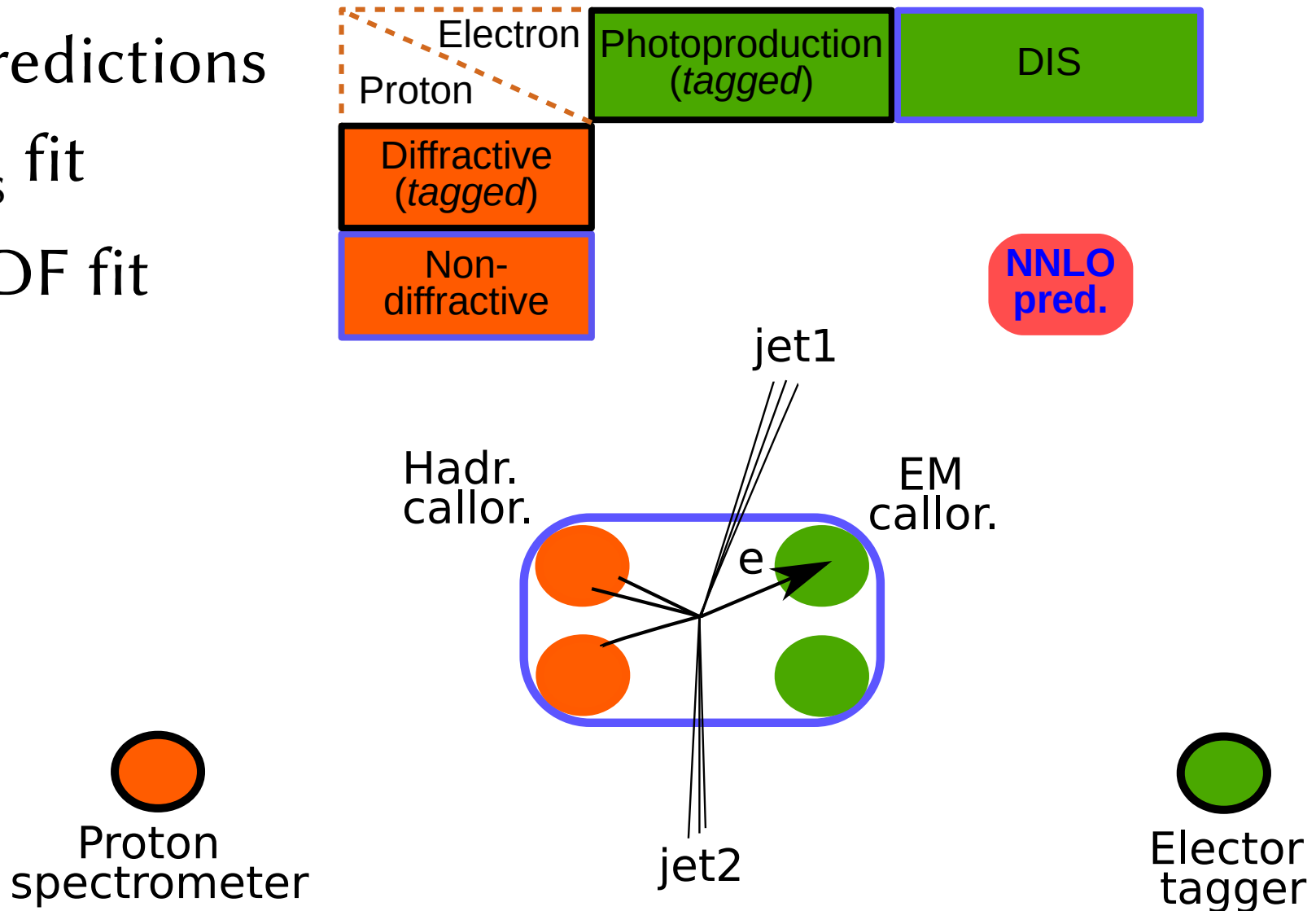


A bit of history

- **1973** Asymptotic freedom of QCD
- **1993** NLO studies of DIS jets
- **2016** NNLO corrections for DIS jets

Jets in DIS at NNLO

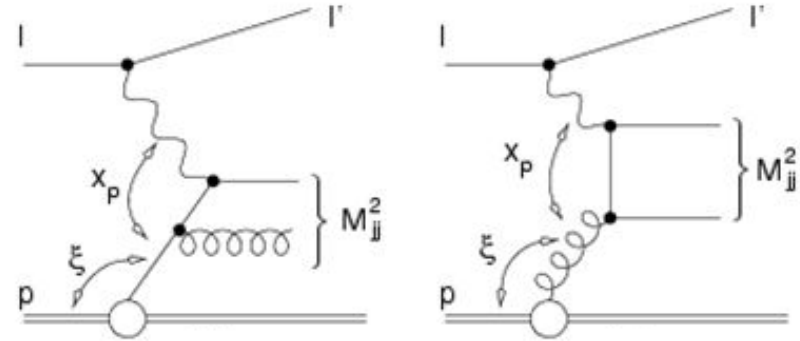
- ✓ Predictions
- ✓ α_s fit
- ✓ PDF fit



NNLO α_S fit of H1 jets data in DIS

Why α_S ?

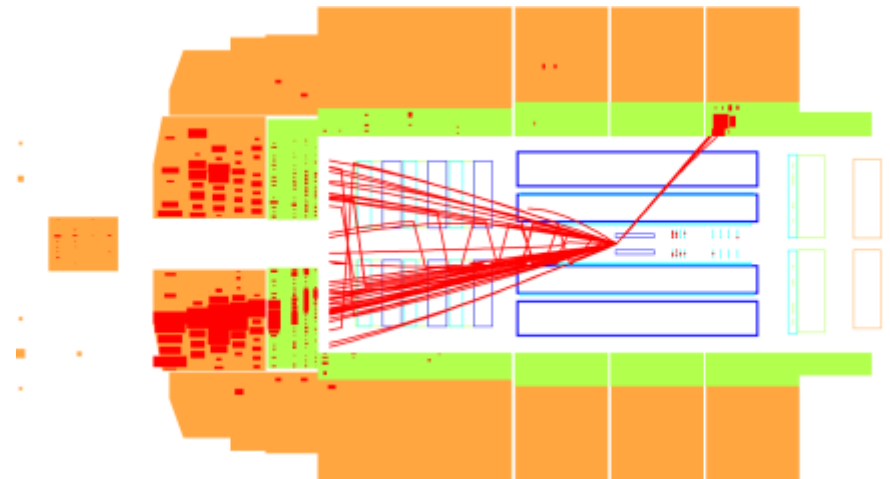
- Among the least known SM parameters
 $G_F = 1.1663787(6) \times 10^{-5} \text{ GeV}^{-2}$
 $\alpha_S = 1.181(11) \times 10^{-1}$ [PDG16]
- Great importance for LHC physics



Dijet DIS production at H1

Why now?

- NNLO revolution in the last years
- NNLO predictions now available for both pp and ep dijets
- Complementary to the α_S extraction in pp at intermediate scales $7 < \mu < 80 \text{ GeV}$



First NNLO α_S fit of the jet ep data

The data-sets used in NNLO QCD analysis

Data set [ref.]	\sqrt{s} [GeV]	\mathcal{L} [pb ⁻¹]	DIS kinematic range	Inclusive jets	Dijets $n_{\text{jets}} \geq 2$
300 GeV [17]	300	33	$150 < Q^2 < 5000 \text{ GeV}^2$ $0.2 < y < 0.6$	$7 < P_{\text{T}}^{\text{jet}} < 50 \text{ GeV}$	$P_{\text{T}}^{\text{jet}} > 7 \text{ GeV}$ $8.5 < \langle P_{\text{T}} \rangle < 35 \text{ GeV}$
HERA-I [23]	319	43.5	$5 < Q^2 < 100 \text{ GeV}^2$ $0.2 < y < 0.7$	$5 < P_{\text{T}}^{\text{jet}} < 80 \text{ GeV}$	$5 < P_{\text{T}}^{\text{jet}} < 50 \text{ GeV}$ $5 < \langle P_{\text{T}} \rangle < 80 \text{ GeV}$ $m_{12} > 18 \text{ GeV}$ $(\langle P_{\text{T}} \rangle > 7 \text{ GeV})^*$
HERA-I [21]	319	65.4	$150 < Q^2 < 15000 \text{ GeV}^2$ $0.2 < y < 0.7$	$5 < P_{\text{T}}^{\text{jet}} < 50 \text{ GeV}$	—
HERA-II [15]	319	290	$5.5 < Q^2 < 80 \text{ GeV}^2$ $0.2 < y < 0.6$	$4.5 < P_{\text{T}}^{\text{jet}} < 50 \text{ GeV}$	$P_{\text{T}}^{\text{jet}} > 4 \text{ GeV}$ $5 < \langle P_{\text{T}} \rangle < 50 \text{ GeV}$
HERA-II [15, 24]	319	351	$150 < Q^2 < 15000 \text{ GeV}^2$ $0.2 < y < 0.7$	$5 < P_{\text{T}}^{\text{jet}} < 50 \text{ GeV}$	$5 < P_{\text{T}}^{\text{jet}} < 50 \text{ GeV}$ $7 < \langle P_{\text{T}} \rangle < 50 \text{ GeV}$ $m_{12} > 16 \text{ GeV}$

Inclusive jets (H1 HERA-II)

Double-diff.

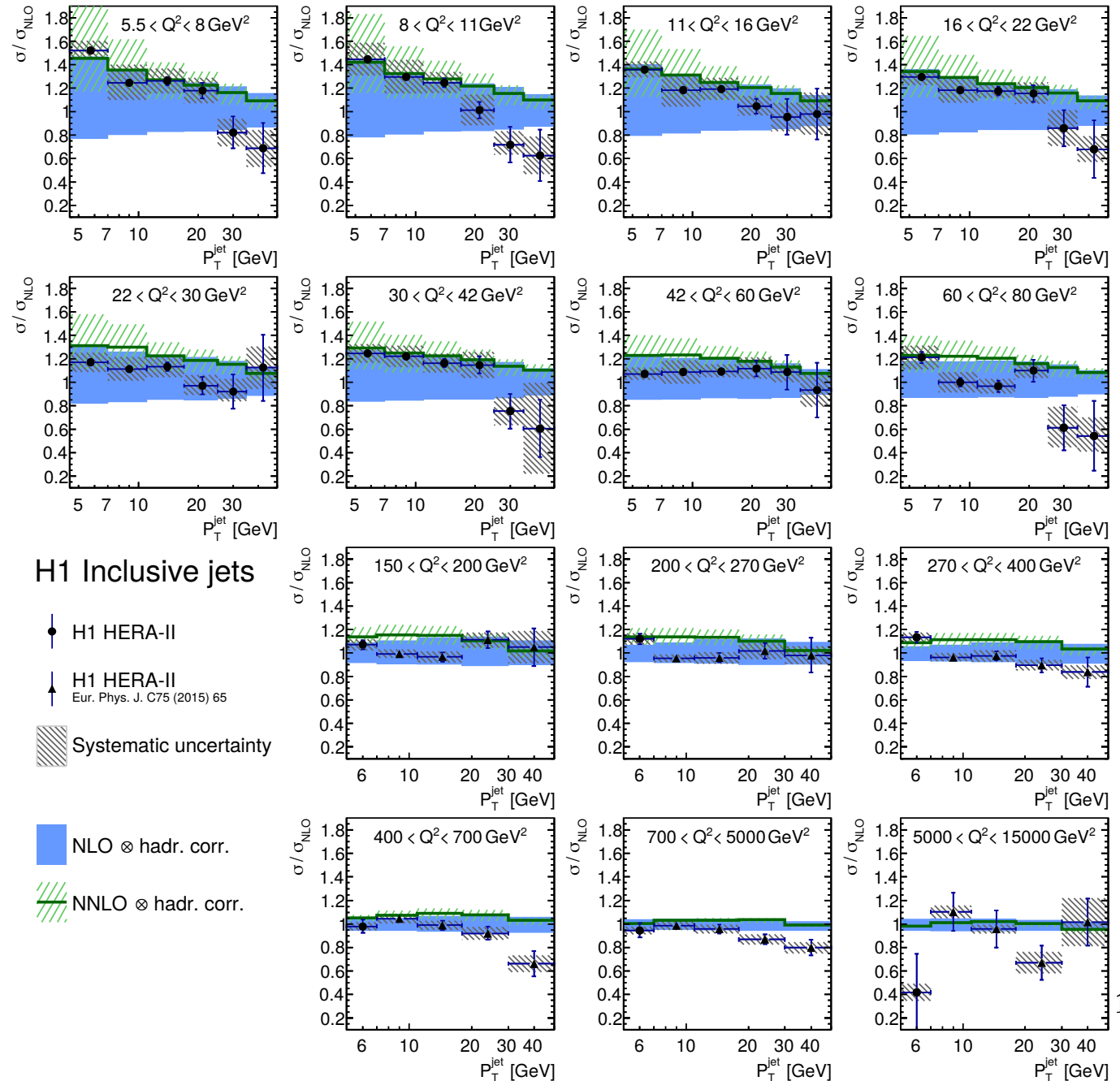
- Q^2 and p_T^{jet}
- Phase space:
 $0.2 < y < 0.6$
 $-1 < \eta_{\text{lab}}^{\text{jet}} < 2.5$
 jets found in $\gamma^* p$
 with k_T algo ($R=1$)

NLO predictions

- *NNPDF 3.0 NLO*
- Larger scale unc.
- $\text{Chi2/ndf} = 1.7$

NNLO predictions

- *NNPDF 3.0 NNLO*
- Smaller scale unc.
- $\text{Chi2/ndf} = 1.3$



Dijets (H1 HERA-II)

Double-diff.

- Q^2 and $\langle p_T \rangle_2$

- Mean dijet p_T

$$\langle p_T \rangle_2 = \frac{p_T^{\text{jet1}} + p_T^{\text{jet2}}}{2}$$

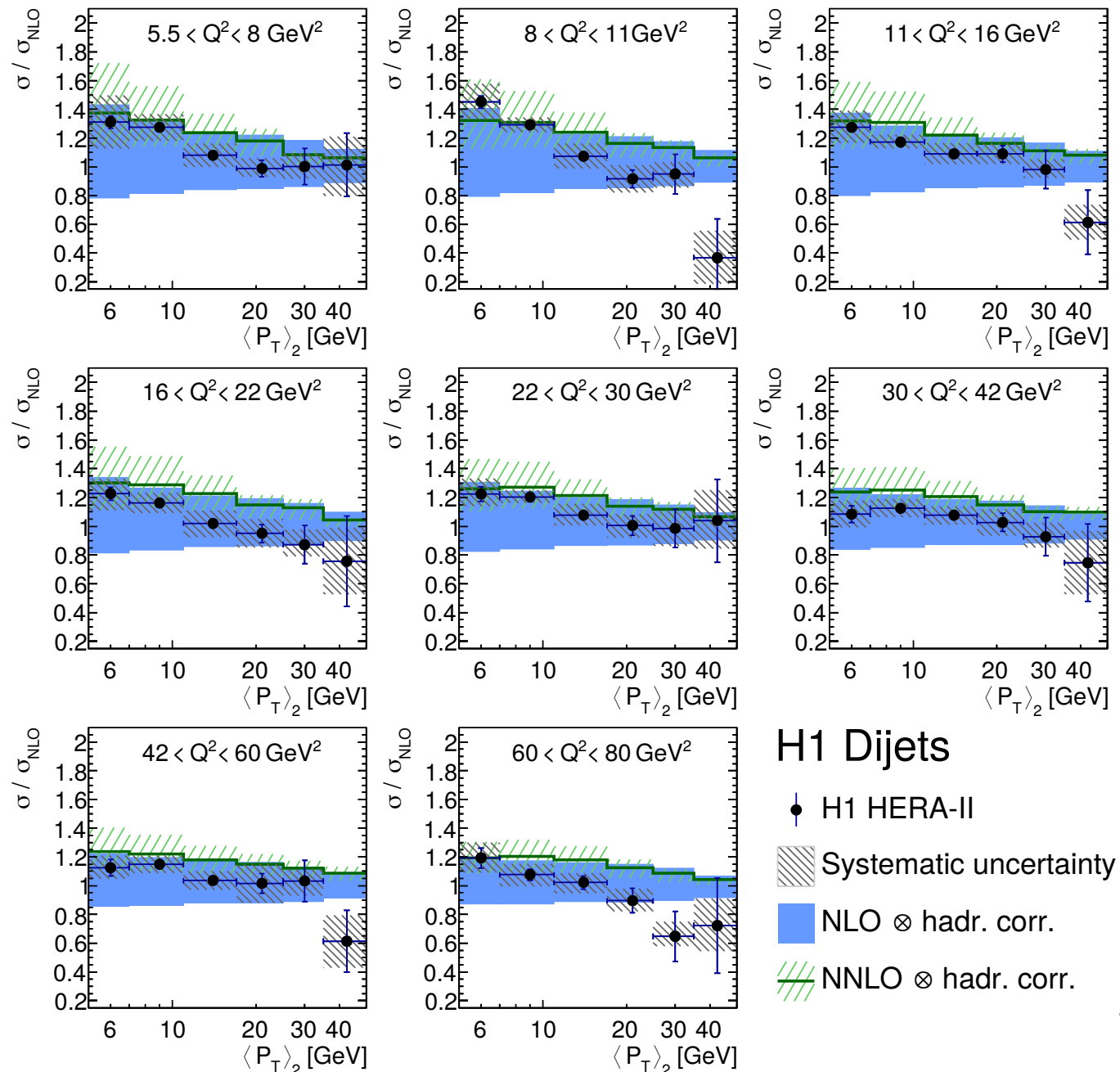
jets found in $\gamma^* p$
with k_T algo ($R=1$)

NLO predictions

- NNPDF 3.0 NLO
- Larger scale unc.
- $\text{Chi2/ndf} = 1.4$

NNLO predictions

- NNPDF 3.0 NNLO
- Smaller scale unc.
- $\text{Chi2/ndf} = 0.6$

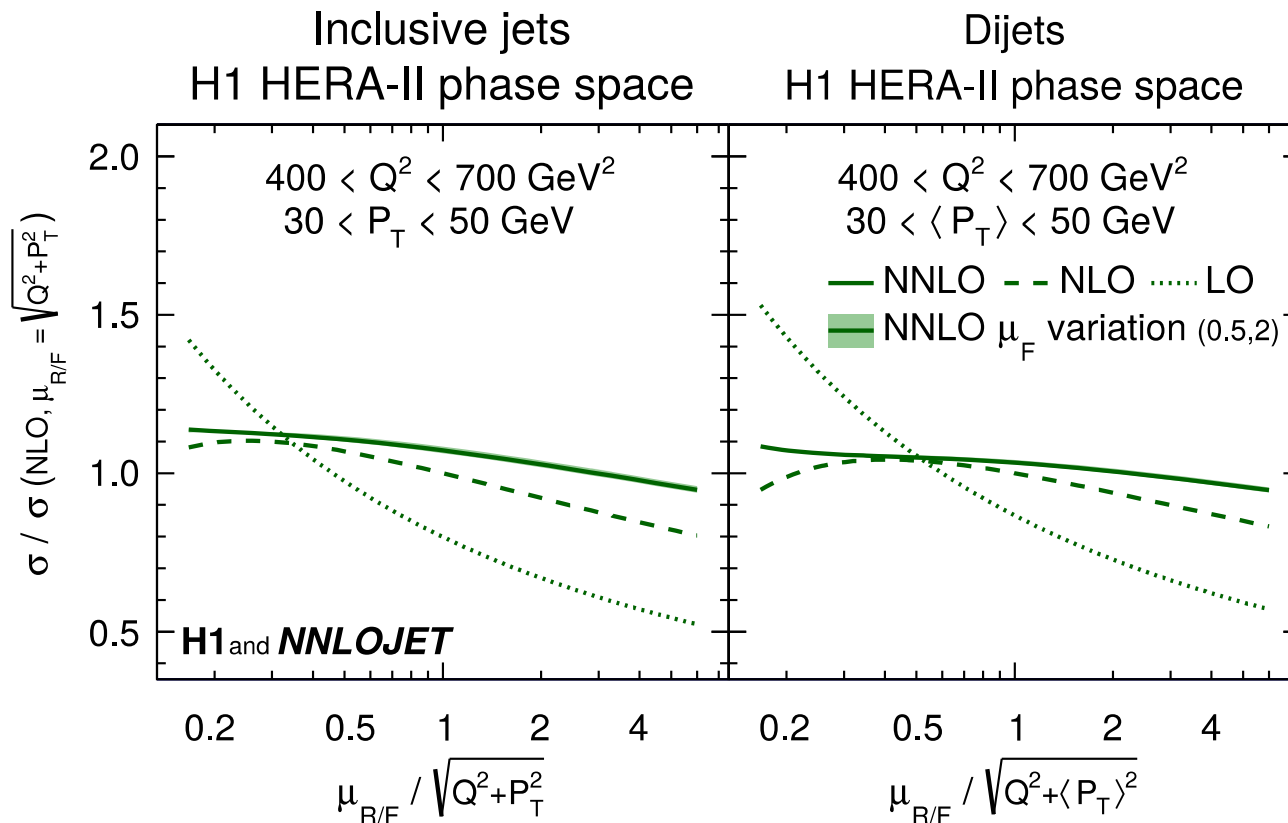


H1 Dijets

Scale dependence

- The NNLO predictions depend **less** on the renormalization scale (=have smaller theor. unc.)
- To estimate the uncertainty the scale varied up and down by the factor of 2

- As a scale we use $\mu_R = \mu_F = \sqrt{Q^2 + p_T^2}$ Others functional forms also tested



Functional form of the scale

- 7 possible function studied
- NNLO α_s is typically smaller than the NLO one
- The NNLO χ^2 is typically better
- NNLO scale unc. is smaller

$$\mu^2 = Q^2$$

$$\mu^2 = p_T^2$$

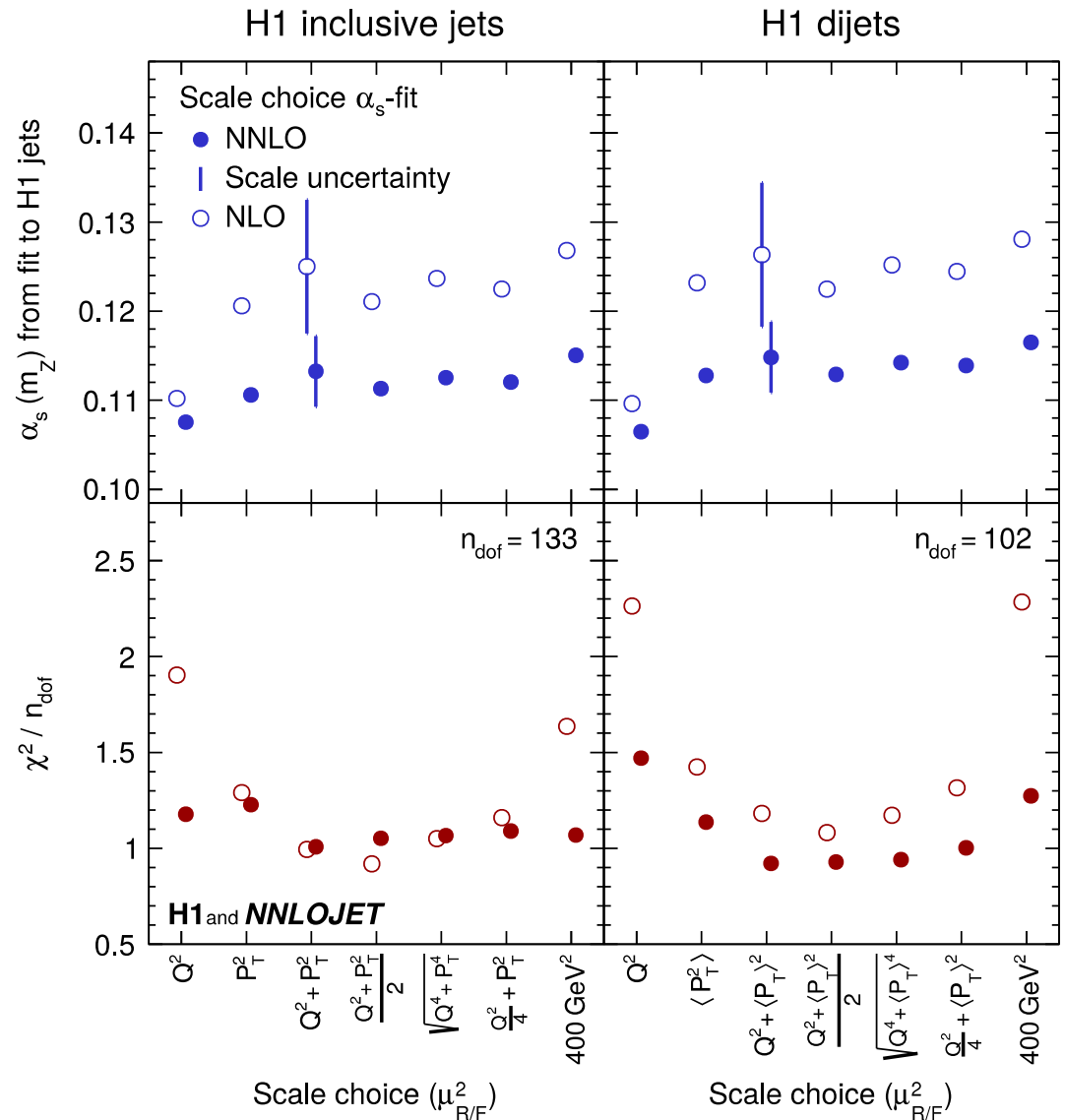
$$\mu^2 = Q^2 + p_T^2$$

$$\mu^2 = \frac{Q^2 + p_T^2}{2}$$

$$\mu^2 = \sqrt{Q^4 + p_T^4}$$

$$\mu^2 = Q^2/4 + p_T^2$$

$$\mu^2 = 400 \text{ GeV}^2$$



All data above m_b threshold used

α_S in PDF and α_S in ME

- Alpha strong affects both, PDFs and matrix element
- Both effects considered, α_S in ME more prominent

$$\sigma_i = \sum_{k=g,q,\bar{q}} \int dx f_k(x, \mu_F) \hat{\sigma}_{i,k}(x, \mu_R, \mu_F) \cdot c_{\text{had},i}$$

α_S dep.
 α_S dep.

$$\hat{\sigma}_{i,k}(x, \mu_R, \mu_F) = \sum_n \alpha_S^n(\mu_R) \hat{\sigma}_{i,k}^{(n)}(x, \mu_R, \mu_F)$$

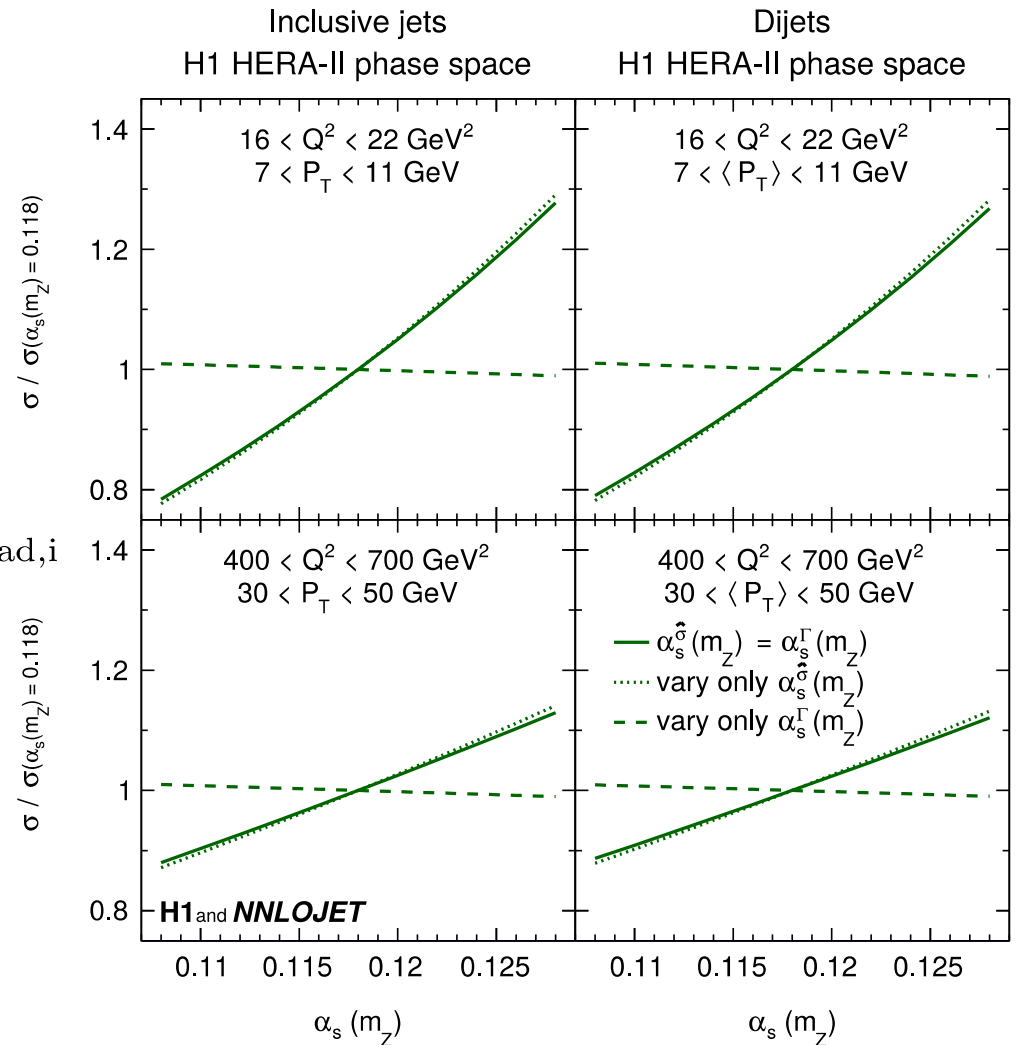
DGLAP equations

$$\mu_F^2 \frac{df}{d\mu_F^2} = P(z, \alpha_S) \otimes f(x, \mu_F^2)$$

PDFs at scale $\mu_0 = 20$ GeV very well constrained by lot of data
 $\rightarrow \alpha_S$ - “independent”

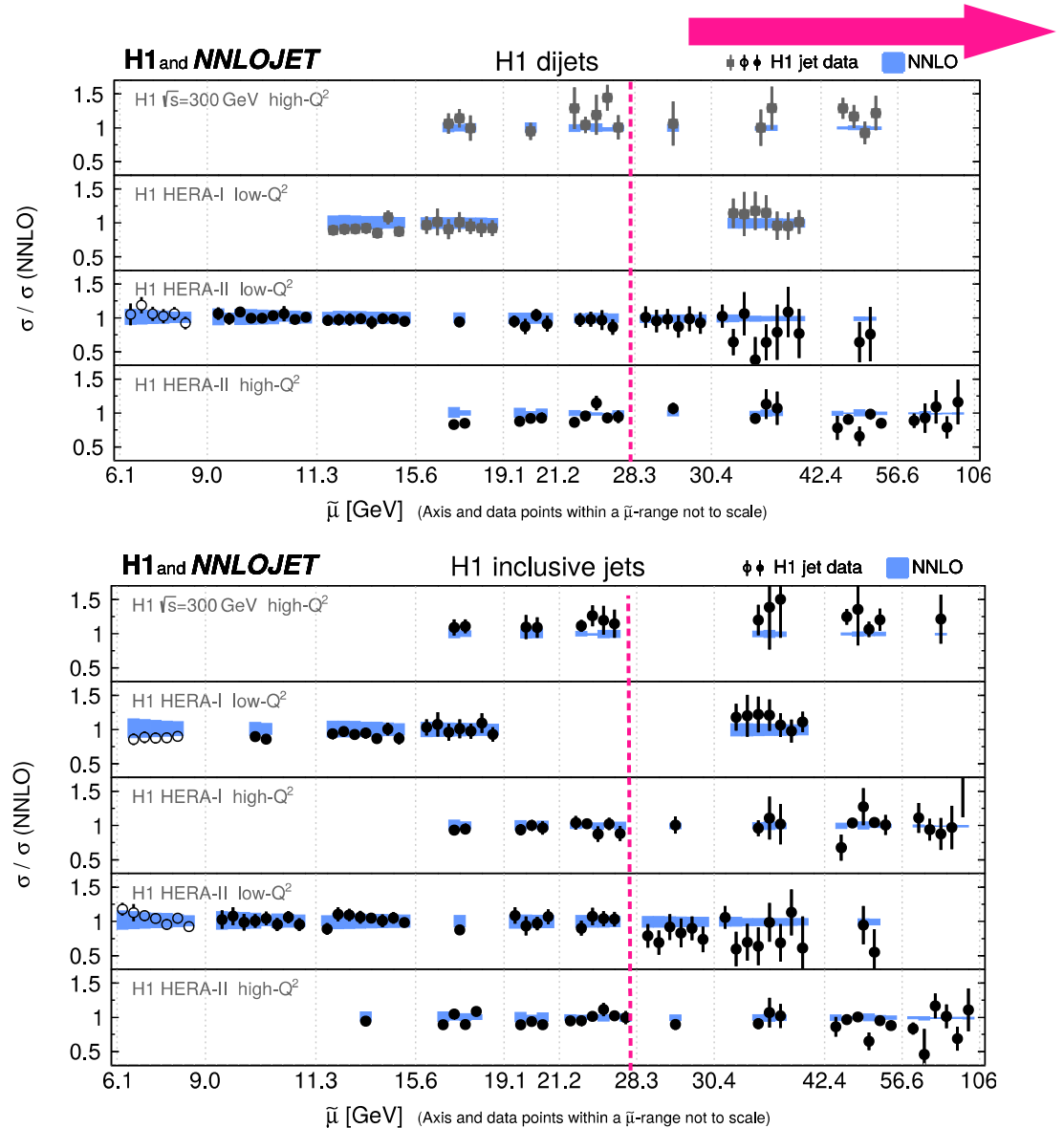
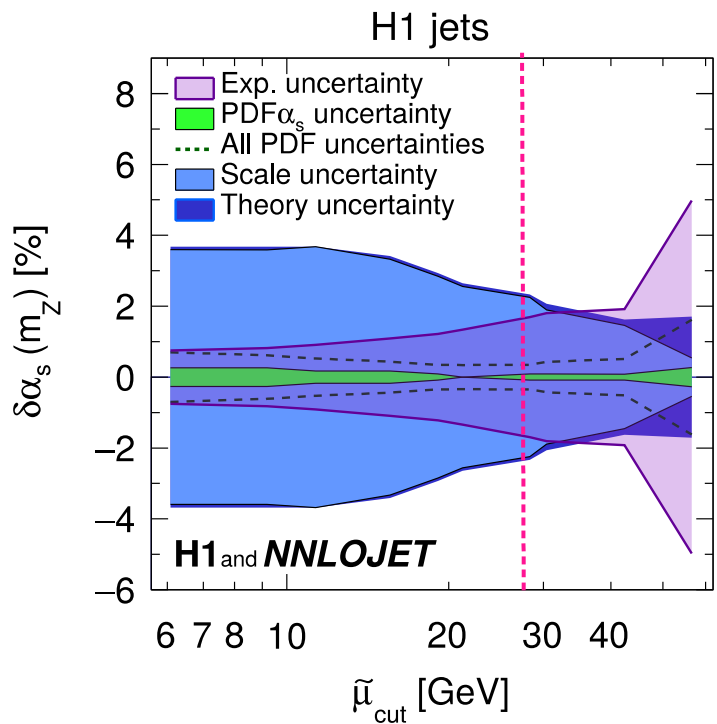


Original PDFs at scale $\mu_0 = 20$ GeV evolved to higher/lower scales by DGLAP with $\alpha_S = \alpha_S(\text{fit par.})$



Which data do we use in the fit?

- The scale uncertainty gets higher with smaller scales
 $(\mu = \sqrt{p_T^2 + Q^2})$
- We use only data $\mu > \mu_{\text{cut}}$



Small $\mu_{\text{cut}} \rightarrow$ high theor. unc.
 Large $\mu_{\text{cut}} \rightarrow$ high exp. unc.



Compromise $\mu_{\text{cut}} = 28 \text{ GeV}$

Alpha strong running and central value

$$\alpha_S(m_Z) = 0.1157$$

Data unc. (20)_{exp}

Hadronisation (6)_{had}

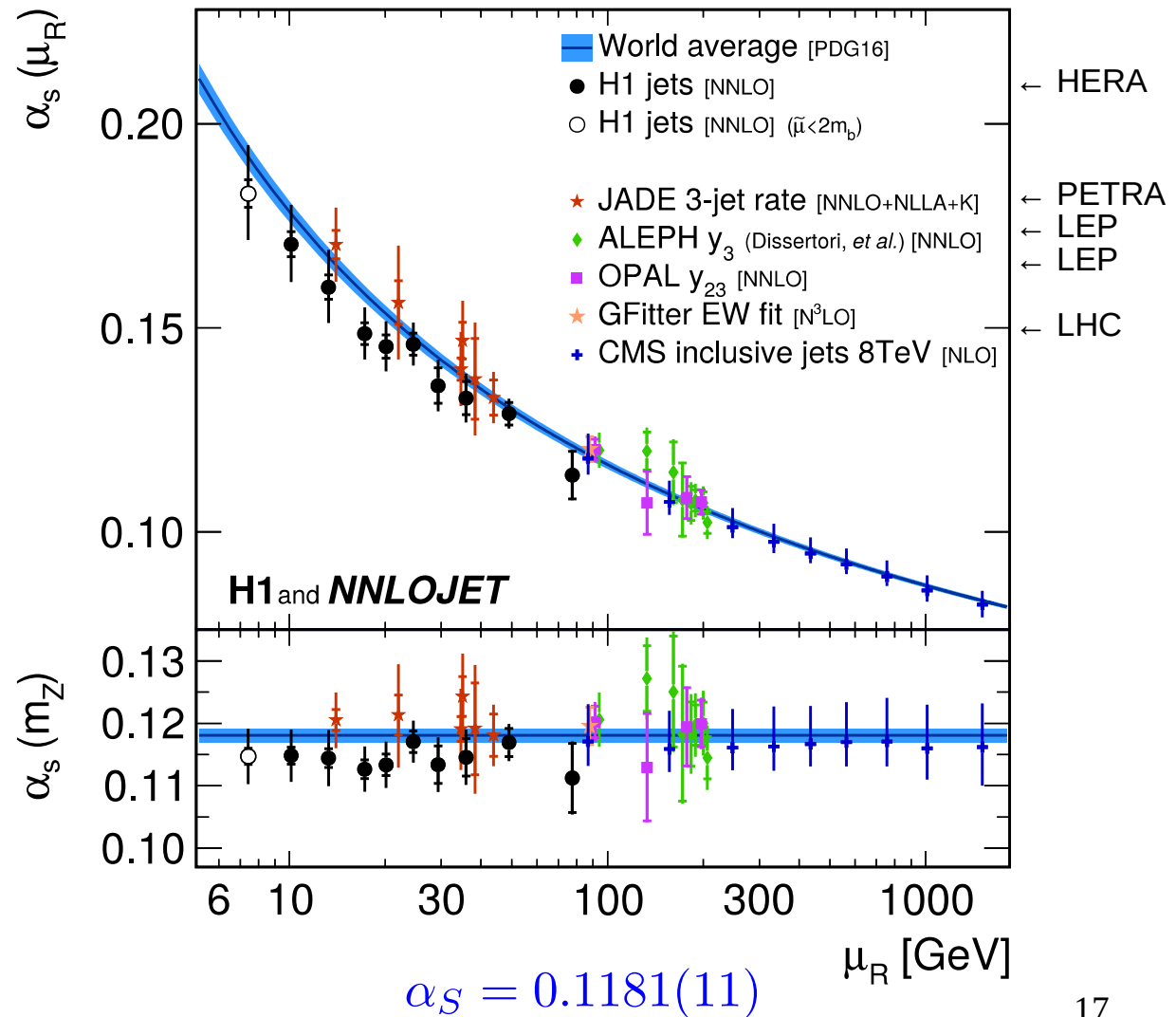
NNPDF 3.1 unc. (3)_{PDF}

α_S^{PDF} variants (2)_{PDF} α_S

PDFs from 5 collab. (3)_{PDFSet}

Scale unc. (27)_{scale}

- Scale and experimental unc. dominant
- Consistent with PDG “world average” value



Simultaneous α_S + PDF fit (H1PDF2017)

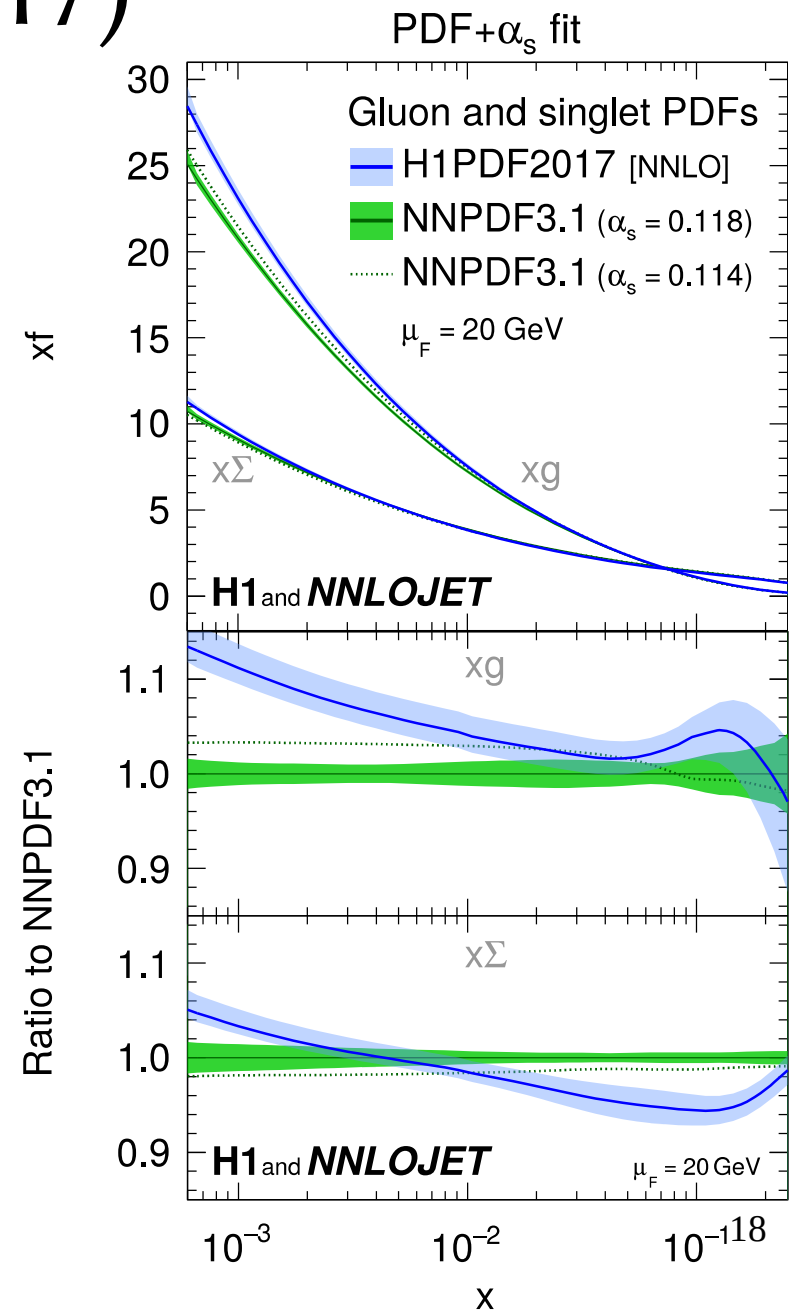
- HERAPDF-like parametrization with 12 parameters at the starting scale $\mu_0^2 = 1.9 \text{ GeV}^2$
- Only data with $Q^2 > 10 \text{ GeV}^2$
- The α_S taken as an additional free parameter of the fit
- Experimental, scale, parametrization and model uncertainty considered

Normalized jet data

Data set [ref.]	Q^2 domain	Inclusive jets	Dijets	Normalised inclusive jets	Normalised dijets	Stat. corr. between samples
300 GeV [17]	high- Q^2	✓	✓	–	–	–
HERA-I [23]	low- Q^2	✓	✓	–	–	–
HERA-I [21]	high- Q^2	✓	–	✓	–	–
HERA-II [15]	low- Q^2	✓	✓	✓	✓	✓
HERA-II [15, 24]	high- Q^2	✓	✓	✓	✓	✓

Inclusive NC+CC

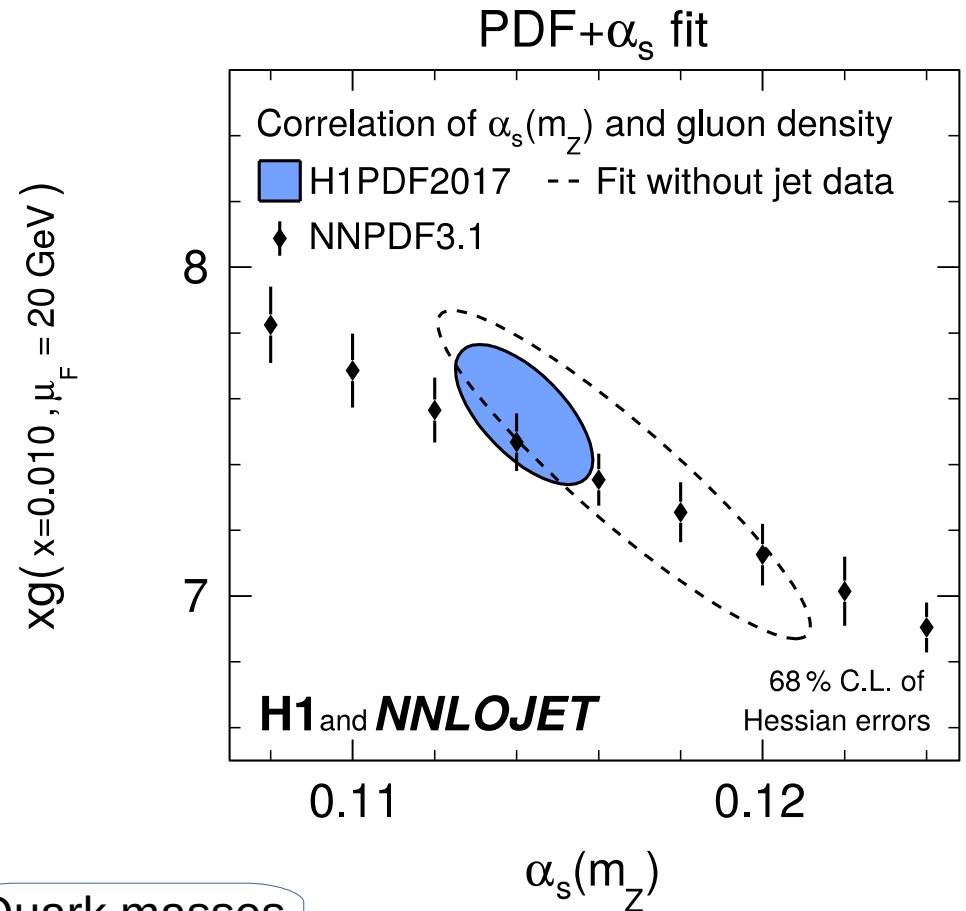
Data set [ref.]	Lepton type	\sqrt{s} [GeV]	Q^2 range [GeV 2]	NC cross sections	CC cross sections	Lepton beam polarisation
Combined low- Q^2 [64]	e^+	301,319	(0.5) 12 – 150	✓	–	–
Combined low- E_p [64]	e^+	225,252	(1.5) 12 – 90	✓	–	–
94 – 97 [61]	e^+	301	150 – 30 000	✓	✓	–
98 – 99 [62, 63]	e^-	319	150 – 30 000	✓	✓	–
99 – 00 [63]	e^+	319	150 – 30 000	✓	✓	–
HERA-II [65]	e^+	319	120 – 30 000	✓	✓	✓
HERA-II [65]	e^-	319	120 – 50 000	✓	✓	✓



Simultaneous PDF + α_S fit

- Resulting fit of inclusive+ jet/inclusive data sets:
 $\chi^2/n_{df} = 1540/(1529 - 13)$
 (with 141 jet data points)
- Anti-correlation between gluon density and α_S
- Huge precision gain by including jet data

→ **Jet data matter**



$$\alpha_S(m_Z) = 0.1142(11)_{\text{exp, had, PDF}} (2)_{\text{mod}} (2)_{\text{par}} (26)_{\text{scale}}$$

Data+had unc.

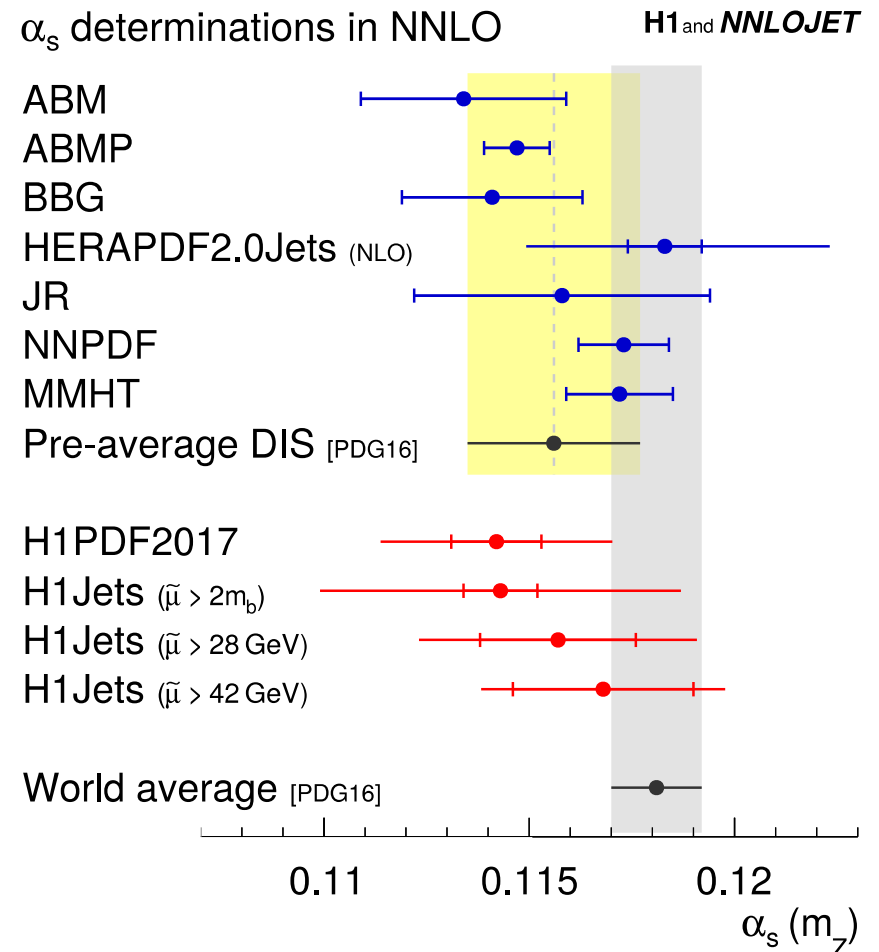
Quark masses
unc.

Parametrization
unc.

From
simultaneous
ren.+fact. scale
variation

Alpha strong values

- Both values of α_S consistent with α_S from global PDF fits
- The NNLO reduces the scale uncertainty **by half**
- The theoretical uncertainty (scale) still dominates
- The indication for lower α_S values when low-scale data included
→ *missing higher orders?*



$$\alpha_S^{\text{H1jets}, \tilde{\mu} > 28 \text{ GeV}}(m_Z) = 0.1157(20)_{\text{exp}}(28)_{\text{theor.}}$$

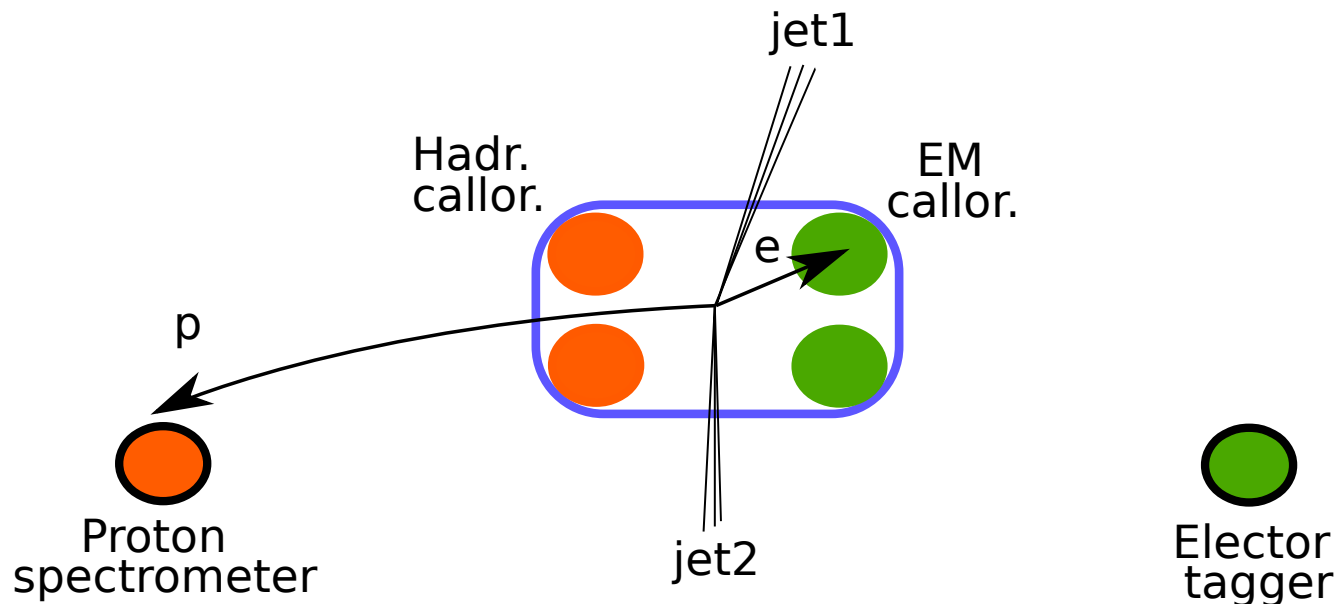
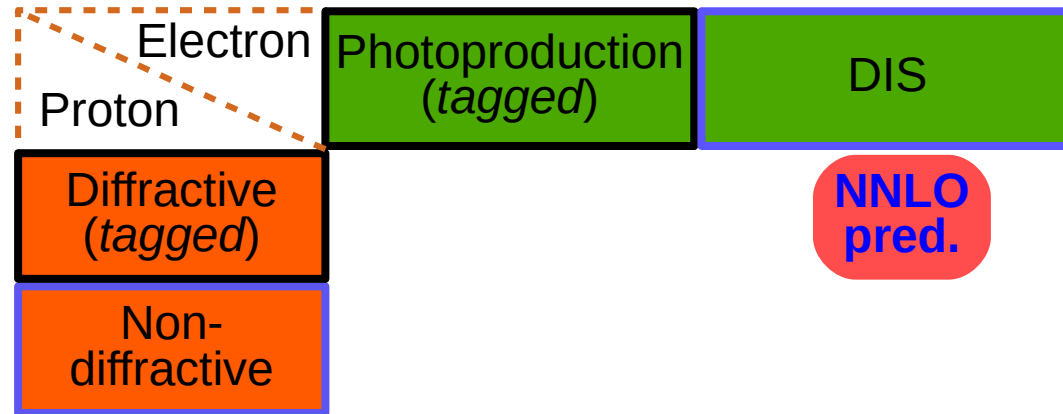
$$\alpha_S^{\text{H1PDF2017}}(m_Z) = 0.1142(11)_{\text{exp}}(26)_{\text{theor.}}$$

Jets in DDIS at NNLO

✓ Predictions

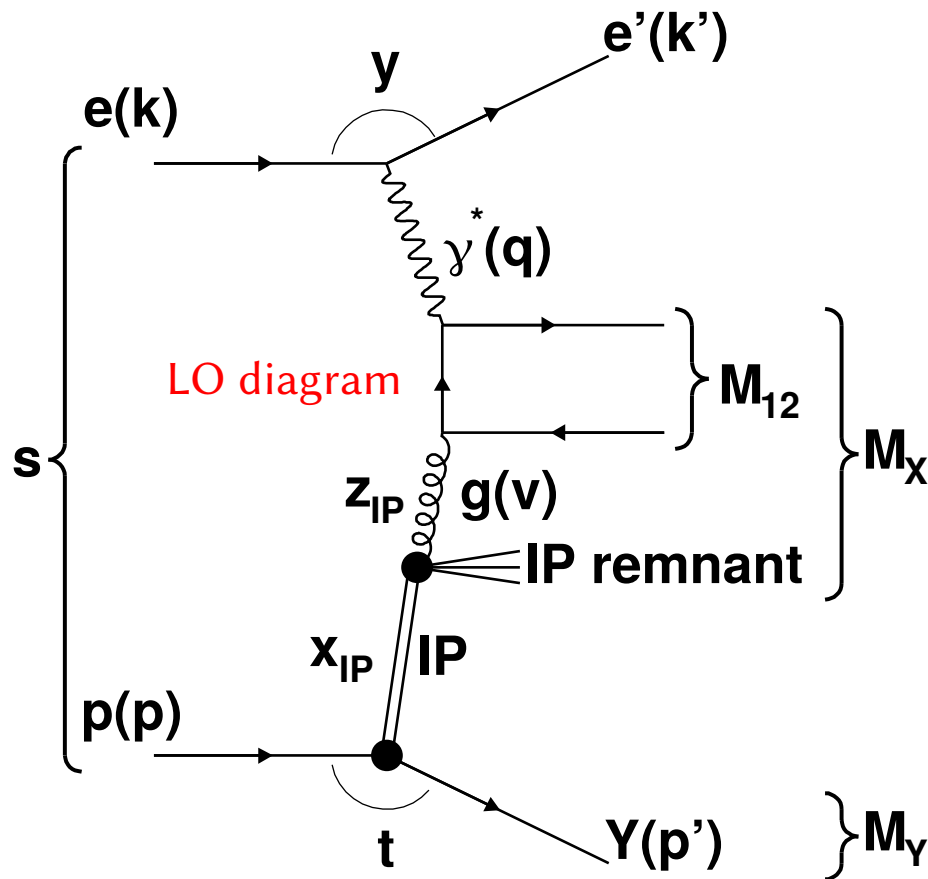
✗ α_s fit

✗ DPDF fit



Diffractive Dijet Production in ep

In diffractive events the beam proton stays intact or dissociates into low mass hadronic system Y



At HERA about 10% of low- x events are diffractive

DIS variables:

$$Q^2 = -(k - k')^2 \quad y = \frac{p \cdot q}{p \cdot k}$$

Dijet mass: M_{12}

Diffractive variables:

$$x_{IP} = 1 - \frac{E'_p}{E_p} \quad t = (p - p')^2$$

At LO: The momentum fraction entering the hard subprocess with respect to the diffractive exchange

$$z_{IP} = \frac{M_{12}^2 + Q^2}{M_X^2 + Q^2}$$

Collinear QCD factorization theorem in hard diffraction

- For diffractive events with a **hard scale** (e.g Q^2 or jets p_T)
- Factorization of the diffractive cross section into **process independent DPDFs** and **partonic cross sections**

$$d\sigma(ep \rightarrow epX) = \sum_i f_i^D(x, Q^2, x_{IP}, t) \otimes d\sigma^{ie}(x, Q^2)$$

- For diffractive processes (including dijets) with Q^2 high enough factorization proven by Collins within perturbative QCD, for low Q^2 factorization breaking suggested

Factorization of Hard Processes in QCD

John C. Collins (IIT, Chicago & SUNY, Stony Brook), Davison E. Soper (Oregon U.), George F. Sterman (SUNY, Stony Brook). May 30, 1989. 91 pp.
Published in *Adv.Ser.Direct.High Energy Phys.* 5 (1989) 1-91
ITP-SB-89-31

DOI: [10.1142/9789814503266_0001](https://doi.org/10.1142/9789814503266_0001)

e-Print: [hep-ph/0409313](https://arxiv.org/abs/hep-ph/0409313) | [PDF](#)

[References](#) | [BibTeX](#) | [LaTeX\(US\)](#) | [LaTeX\(EU\)](#) | [Harvmac](#) | [EndNote](#)
[ADS Abstract Service](#)

[Detailed record](#) - [Cited by 812 records](#) 500+

Proof of factorization for diffractive hard scattering

John C. Collins (Penn State U.). Sep 1997. 12 pp.
Published in *Phys.Rev. D* 57 (1998) 3051-3056, Erratum: *Phys.Rev. D* 61 (2000) 019902

PSU-TH-189

DOI: [10.1103/PhysRevD.57.3051](https://doi.org/10.1103/PhysRevD.57.3051), [10.1103/PhysRevD.61.019902](https://doi.org/10.1103/PhysRevD.61.019902)

e-Print: [hep-ph/9709499](https://arxiv.org/abs/hep-ph/9709499) | [PDF](#)

[References](#) | [BibTeX](#) | [LaTeX\(US\)](#) | [LaTeX\(EU\)](#) | [Harvmac](#) | [EndNote](#)
[ADS Abstract Service](#); [OSTI.gov Server](#)

[Detailed record](#) - [Cited by 404 records](#) 250+

NLO DPDFs

- DPDF sets differ mainly in gluon component which is weakly constrained from inclusive diffractive data
- For gluon dominated diffractive dijet production we have sizable DPDF uncertainty
- DPDFs obey standard DGLAP evolution equation

Fits of **inclusive** data

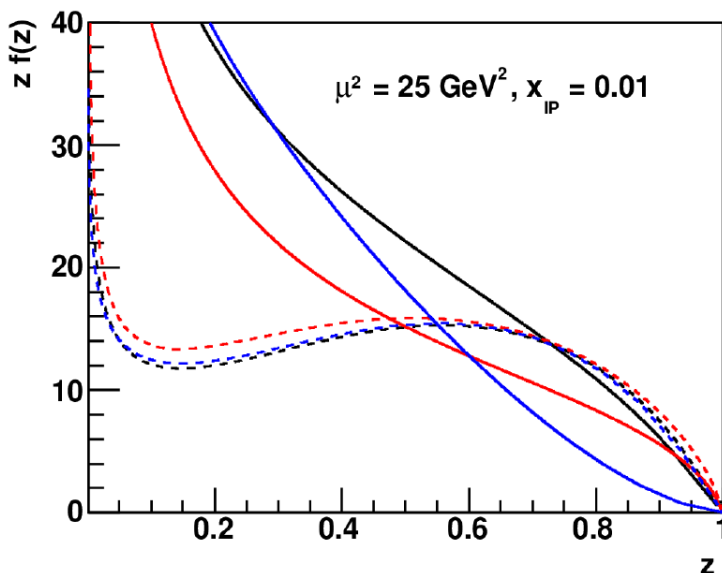
~~H1 2006 Fit A~~
H1 2006 Fit B
 MRW DPDF

Combined **inclusive + dijets** data fits

H1 2007 Fit Jets
 ZEUS 2009 Fit SJ

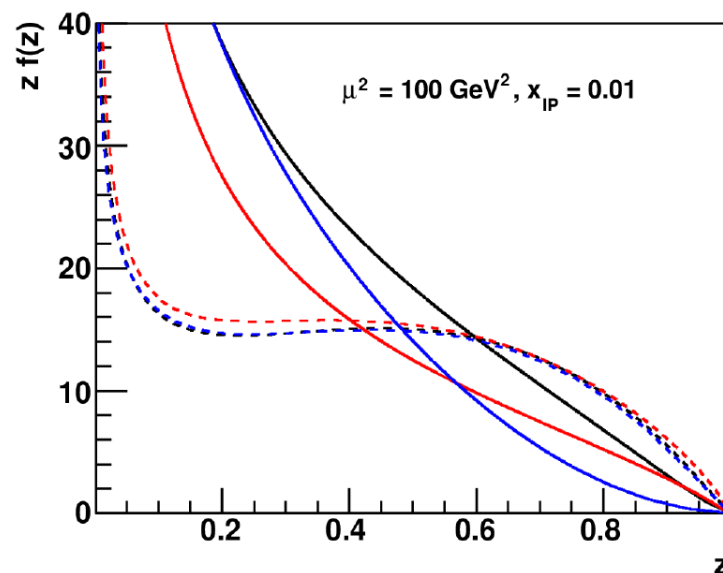
Quark Singlet Densities

----- H1 Fit B - $z \Sigma(z)$
 - - - - H1 Fit Jets - $z \Sigma(z)$
 - - - - ZEUS SJ - $z \Sigma(z) \times 1.2$



Gluon Densities

—— H1 Fit B - $z G(z)$
 — H1 Fit Jets - $z G(z)$
 — ZEUS SJ - $z G(z) \times 1.2$



70% of diffractive exchange momentum carried by gluons

The DIS dijets measurements

- 5times e+p 27.6 GeV + 920 GeV
1times e+p 27.5 GeV + 820 GeV
- 4times Large rapidity gap selection (LRG)
2times Proton spectrometer (FPS, VFPS)

H1 LRG HERA II Phase Space
$4 < Q^2 < 100 \text{ GeV}^2$ $0.1 < y < 0.7$
$x_P < 0.03$ $ t < 1 \text{ GeV}^2$ $M_Y < 1.6 \text{ GeV}$
$p_{T,1}^* > 5.5 \text{ GeV}$ $p_{T,2}^* > 4.0 \text{ GeV}$ $-1 < \eta_{1,2}^{\text{lab}} < 2$

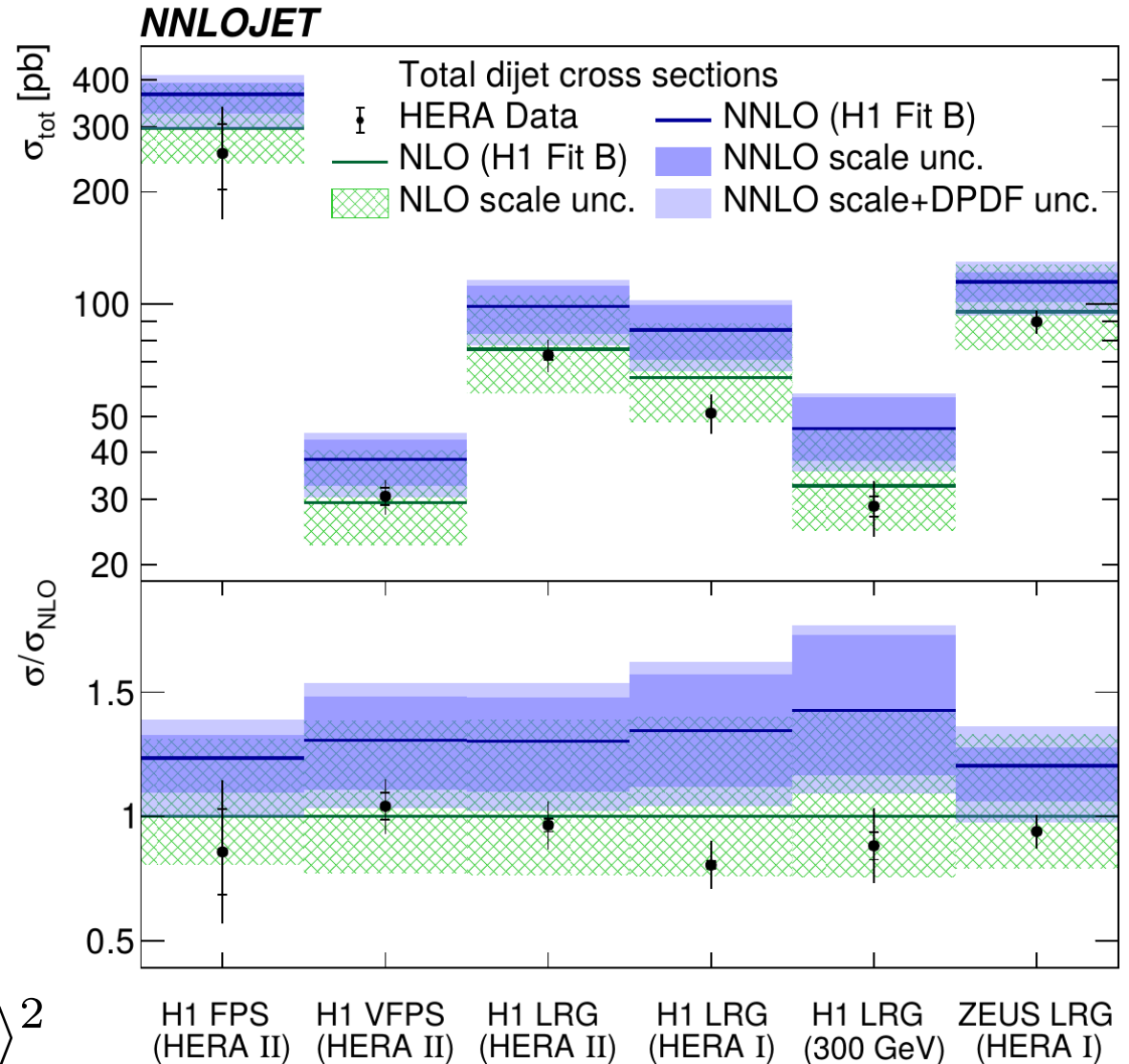


All HERA analyses using k_T -jet algorithm ($R=1$) and asymmetric jet p_T cuts

Total Cross Sections - NLO vs NNLO

- For NNLO the inner bar represents the scale uncertainty, the outer includes DPDF uncertainties
- Total cross sections well described by NLO
- NNLO predictions systematically overestimate the data (NNLO/NLO phase space dependent)

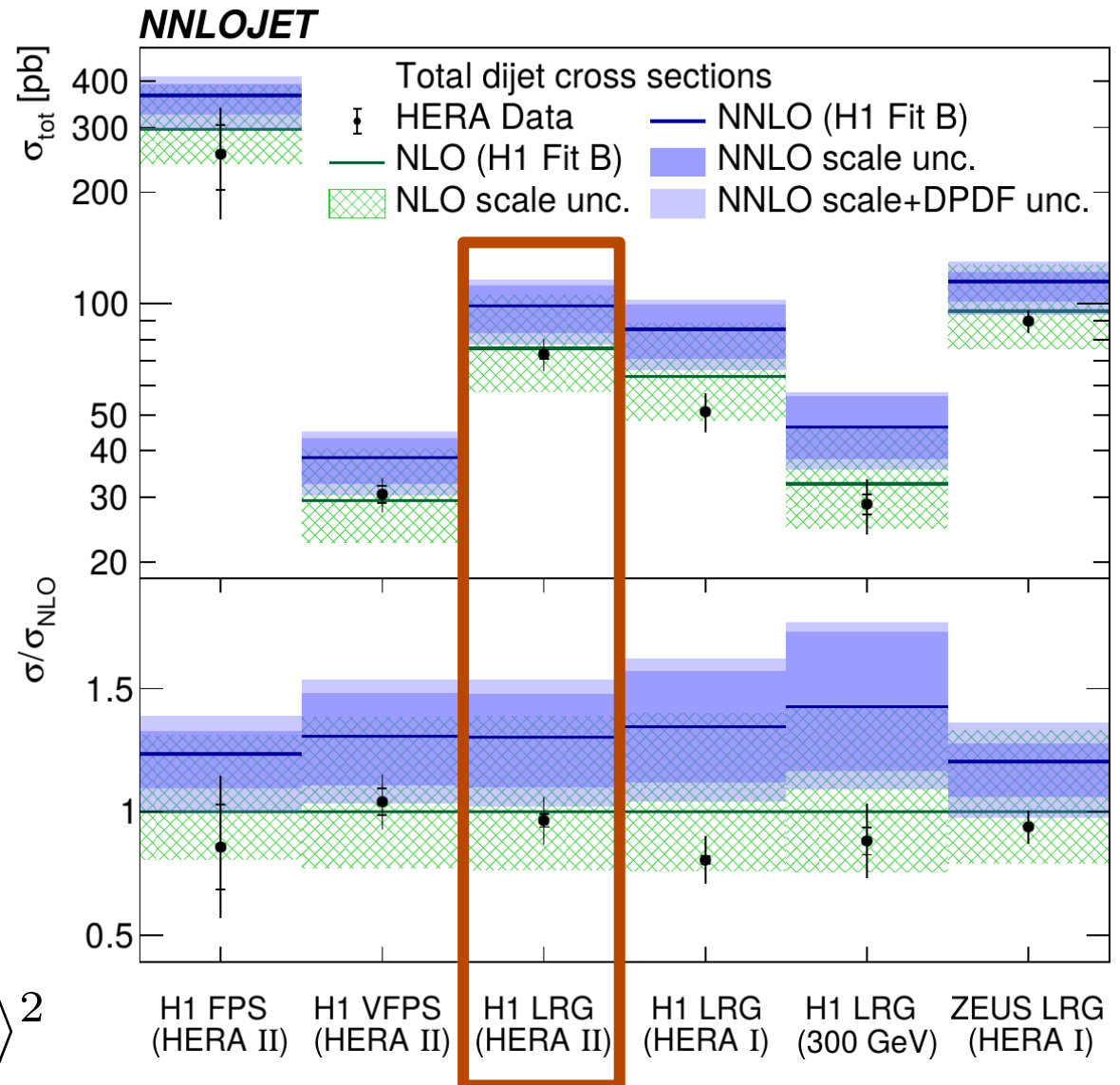
$$\mu_R^2 = \mu_F^2 = Q^2 + \langle p_T^{*jets} \rangle^2$$



Total Cross Sections - NLO vs NNLO

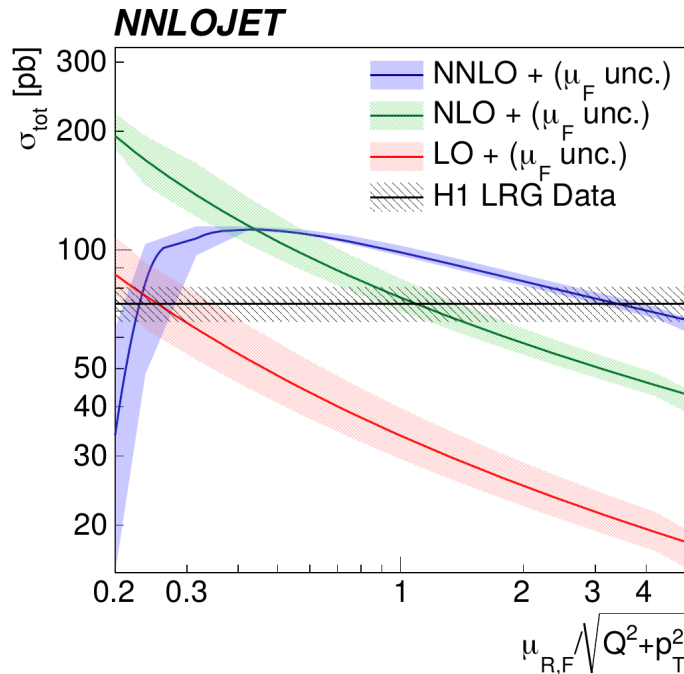
- For NNLO the inner bar represents the scale uncertainty, the outer includes DPDF uncertainties
- Total cross sections well described by NLO
- NNLO predictions systematically overestimate the data (NNLO/NLO phase space dependent)

$$\mu_R^2 = \mu_F^2 = Q^2 + \langle p_T^{*jets} \rangle^2$$



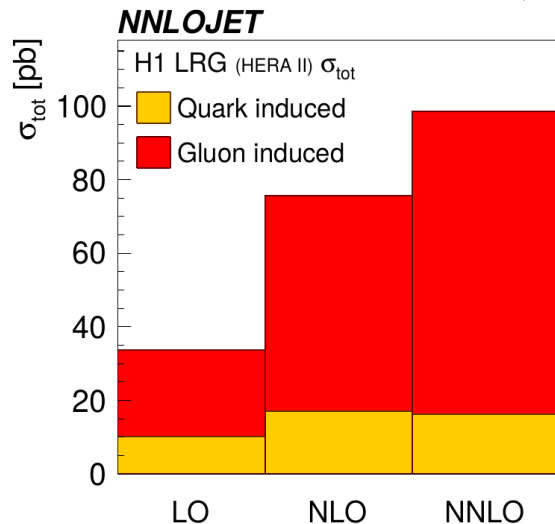
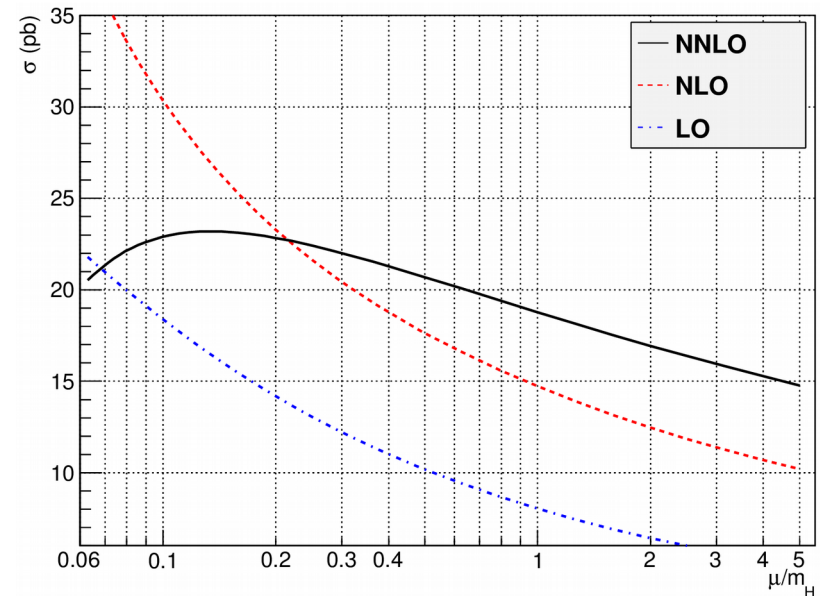
Total Cross Sections - Scale dependence

Jets in DIS ($\sqrt{s} = 320$ GeV)



Higgs production in pp ($\sqrt{s} = 8$ TeV)

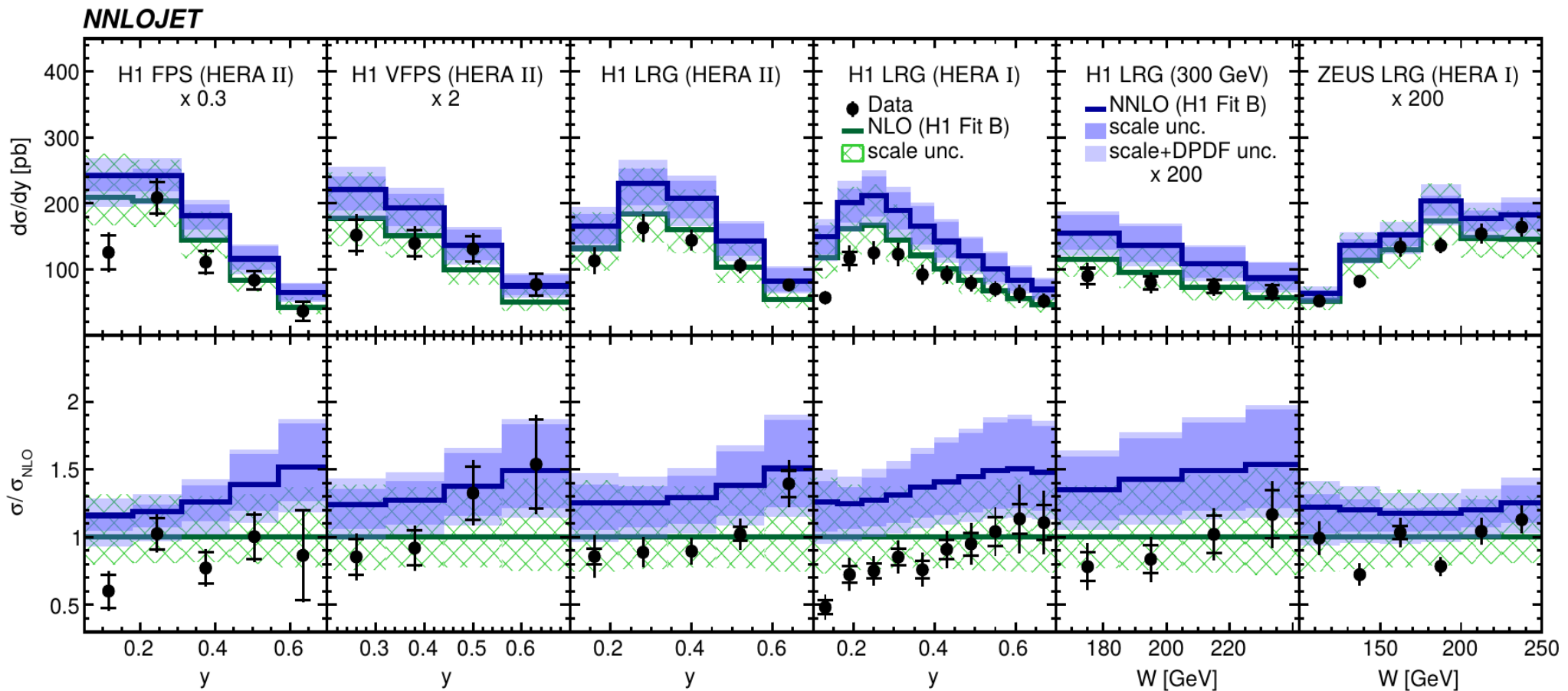
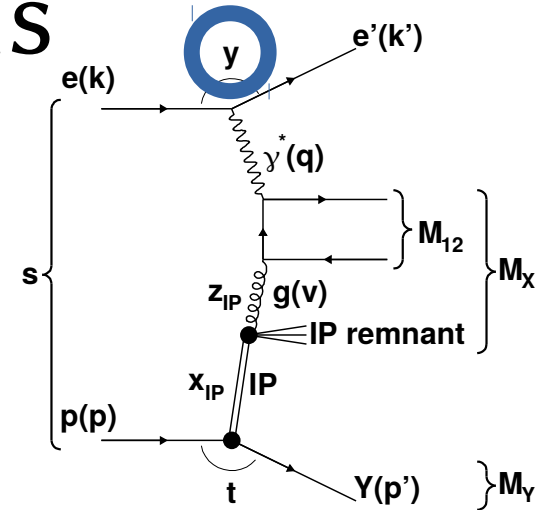
JHEP 1204 (2012) 004



- The gluon-DPDF induced cross section rises gradually with order
- The quark-Induced cross section stagnates at NLO
- At NNLO 84% of the cross section is from gluon DPDF

Differential x-sections

- The same or similar distributions from various analyses grouped into one plot, as shown bellow.
- For inelasticity y NNLO higher for higher y , similar trend in data, note $W = \sqrt{ys}$



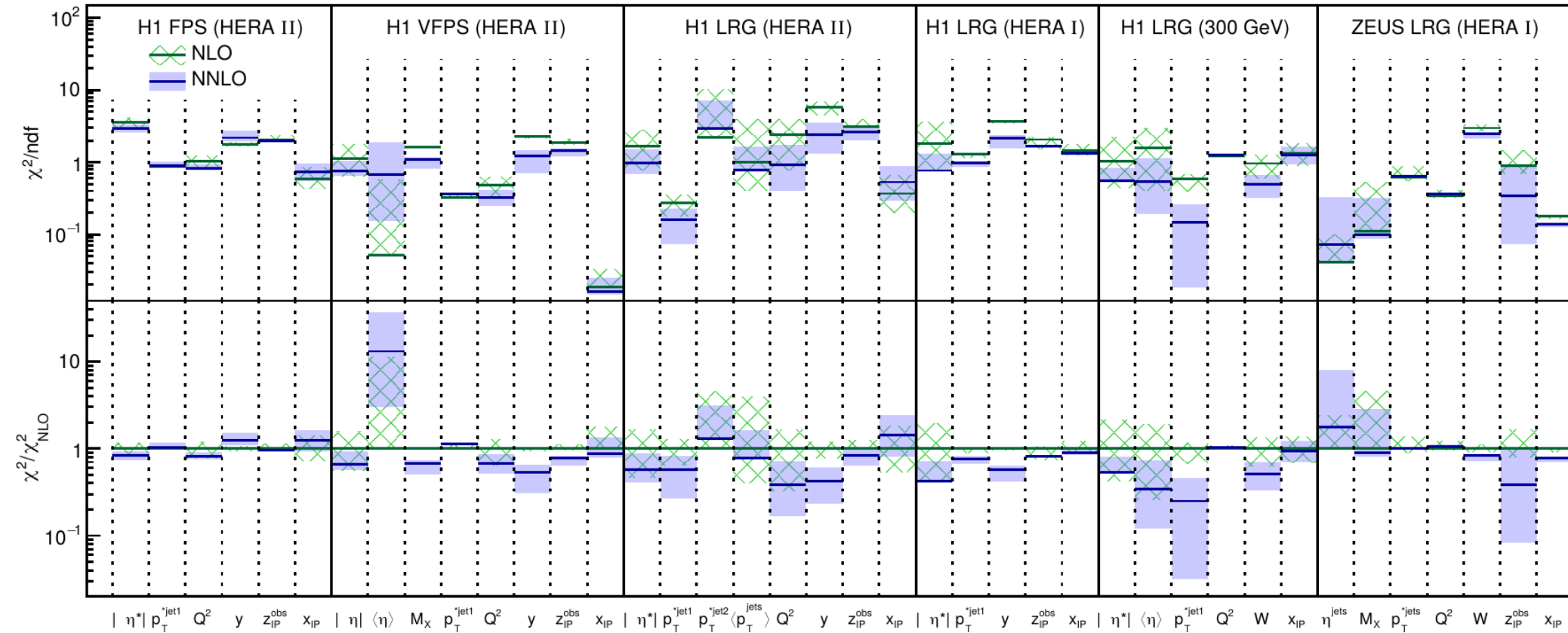
Chi² comparison

- The NNLO typically describe shapes better (improvement seen for all studied DPDFs)

The normalization-independent definition

$$\chi^2 = \min_K \sum_{i,j} \log \frac{\sigma_i^{\text{Data}}}{K \sigma_i^{(\text{N})\text{NLO}}} (V^{-1})_{ij} \log \frac{\sigma_j^{\text{Data}}}{K \sigma_j^{(\text{N})\text{NLO}}}$$

NNLOJET



Conclusion

- The NNLO predictions available for the first time for jets in (D)DIS
- Comparing to NLO the scale uncertainties are smaller and x-sections typically larger

α_s fit of DIS jets

Subclass	$\alpha_s(M_Z^2)$
τ -decays	0.1192 ± 0.0018
lattice QCD	0.1188 ± 0.0011
structure functions	0.1156 ± 0.0021
e^+e^- [jets & shps]	0.1169 ± 0.0034
hadron collider	$0.1151^{+0.0028}_{-0.0027}$
ew precision fits	0.1196 ± 0.0030

H1 NNLO jets 0.1157 ± 0.0034
H1 NNLO jets+PDF 0.1142 ± 0.0028

Pred. for DDIS jets

- Better description of shapes with NNLO, but normalization off
- Only NLO DPDFs available
- Plan for new combined (inclusive+jet) DPDF fit at NNLO

Thank you for your attention



Backup

$\alpha_s(m_Z)$ values from H1 jet cross sections

Data	$\tilde{\mu}_{\text{cut}}$	$\alpha_s(m_Z)$ with uncertainties	th	tot	χ^2/n_{dof}
Inclusive jets					
300 GeV high- Q^2	$2m_b$	0.1221 (31) _{exp} (22) _{had} (5) _{PDF} (3) _{PDFα_s} (4) _{PDFset} (36) _{scale}	(43) _{th}	(53) _{tot}	6.5/15
HERA-I low- Q^2	$2m_b$	0.1093 (17) _{exp} (8) _{had} (5) _{PDF} (5) _{PDFα_s} (7) _{PDFset} (33) _{scale}	(35) _{th}	(39) _{tot}	17.5/22
HERA-I high- Q^2	$2m_b$	0.1136 (24) _{exp} (9) _{had} (6) _{PDF} (4) _{PDFα_s} (4) _{PDFset} (31) _{scale}	(33) _{th}	(41) _{tot}	14.7/23
HERA-II low- Q^2	$2m_b$	0.1187 (18) _{exp} (8) _{had} (4) _{PDF} (4) _{PDFα_s} (3) _{PDFset} (45) _{scale}	(46) _{th}	(50) _{tot}	29.6/40
HERA-II high- Q^2	$2m_b$	0.1121 (18) _{exp} (9) _{had} (5) _{PDF} (4) _{PDFα_s} (2) _{PDFset} (35) _{scale}	(37) _{th}	(41) _{tot}	42.5/29
Dijets					
300 GeV high- Q^2	$2m_b$	0.1213 (39) _{exp} (17) _{had} (5) _{PDF} (2) _{PDFα_s} (3) _{PDFset} (31) _{scale}	(35) _{th}	(52) _{tot}	13.6/15
HERA-I low- Q^2	$2m_b$	0.1101 (23) _{exp} (8) _{had} (5) _{PDF} (4) _{PDFα_s} (5) _{PDFset} (36) _{scale}	(38) _{th}	(45) _{tot}	10.4/20
HERA-II low- Q^2	$2m_b$	0.1173 (14) _{exp} (9) _{had} (5) _{PDF} (5) _{PDFα_s} (3) _{PDFset} (44) _{scale}	(45) _{th}	(47) _{tot}	17.4/41
HERA-II high- Q^2	$2m_b$	0.1089 (21) _{exp} (7) _{had} (5) _{PDF} (3) _{PDFα_s} (3) _{PDFset} (25) _{scale}	(27) _{th}	(34) _{tot}	28.0/23
H1 inclusive jets	$2m_b$	0.1132 (10) _{exp} (5) _{had} (4) _{PDF} (4) _{PDFα_s} (2) _{PDFset} (40) _{scale}	(40) _{th}	(42) _{tot}	134.0/133
H1 inclusive jets	28 GeV	0.1152 (20) _{exp} (6) _{had} (2) _{PDF} (2) _{PDFα_s} (3) _{PDFset} (26) _{scale}	(27) _{th}	(33) _{tot}	44.1/60
H1 dijets	$2m_b$	0.1148 (11) _{exp} (6) _{had} (5) _{PDF} (4) _{PDFα_s} (4) _{PDFset} (40) _{scale}	(41) _{th}	(42) _{tot}	93.9/102
H1 dijets	28 GeV	0.1147 (24) _{exp} (5) _{had} (3) _{PDF} (2) _{PDFα_s} (3) _{PDFset} (24) _{scale}	(25) _{th}	(35) _{tot}	30.8/43
H1 jets	$2m_b$	0.1143 (9) _{exp} (6) _{had} (5) _{PDF} (5) _{PDFα_s} (4) _{PDFset} (42) _{scale}	(43) _{th}	(44) _{tot}	195.0/199
H1 jets	28 GeV	0.1157 (20) _{exp} (6) _{had} (3) _{PDF} (2) _{PDFα_s} (3) _{PDFset} (27) _{scale}	(28) _{th}	(34) _{tot}	63.2/90
H1 jets	42 GeV	0.1168 (22) _{exp} (7) _{had} (2) _{PDF} (2) _{PDFα_s} (5) _{PDFset} (17) _{scale}	(20) _{th}	(30) _{tot}	37.6/40
H1PDF2017 [NNLO]	$2m_b$	0.1142 (11) _{exp,NP,PDF} (2) _{mod} (2) _{par} (26) _{scale}		(28) _{tot}	1539.7/1516

Running of the strong coupling

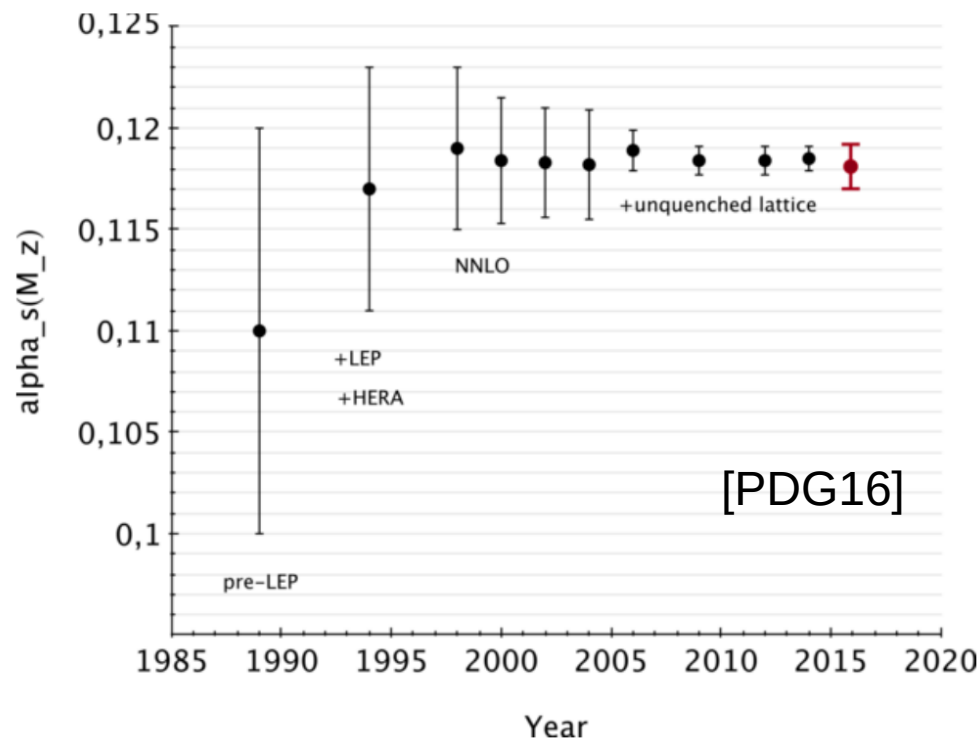
μ_R [GeV]	Inclusive jets		Dijets		H1 jets	
	$\alpha_s(m_Z)$	$\alpha_s(\mu_R)$	$\alpha_s(m_Z)$	$\alpha_s(\mu_R)$	$\alpha_s(m_Z)$	$\alpha_s(\mu_R)$
7.4	0.1148 (13) (42)	0.1830 (34) (114)	0.1182 (28) (41)	0.1923 (77) (116)	0.1147 (13) (43)	0.1829 (34) (114)
10.1	0.1136 (17) (36)	0.1678 (39) (81)	0.1169 (14) (42)	0.1751 (34) (99)	0.1148 (14) (40)	0.1705 (31) (91)
13.3	0.1147 (15) (43)	0.1605 (30) (88)	0.1131 (18) (38)	0.1573 (36) (76)	0.1144 (15) (42)	0.1600 (30) (86)
17.2	0.1130 (15) (33)	0.1492 (26) (59)	0.1104 (19) (30)	0.1445 (33) (53)	0.1127 (15) (33)	0.1486 (27) (59)
20.1	0.1136 (17) (33)	0.1457 (29) (56)	0.1116 (22) (31)	0.1425 (36) (52)	0.1134 (17) (33)	0.1454 (29) (55)
24.5	0.1173 (17) (30)	0.1463 (26) (48)	0.1147 (23) (24)	0.1423 (36) (38)	0.1171 (17) (29)	0.1460 (27) (46)
29.3	0.1084 (36) (29)	0.1287 (51) (41)	0.1163 (34) (34)	0.1401 (50) (50)	0.1134 (30) (32)	0.1358 (44) (46)
36.0	0.1153 (32) (37)	0.1338 (43) (50)	0.1135 (37) (29)	0.1314 (50) (39)	0.1146 (30) (33)	0.1328 (41) (44)
49.0	0.1170 (22) (20)	0.1290 (27) (25)	0.1127 (31) (15)	0.1238 (37) (18)	0.1169 (23) (19)	0.1290 (28) (24)
77.5	0.1111 (55) (19)	0.1137 (58) (20)	0.1074 (84) (19)	0.1099 (88) (20)	0.1113 (55) (19)	0.1139 (58) (20)

Results for the PDF+ α_s -fit

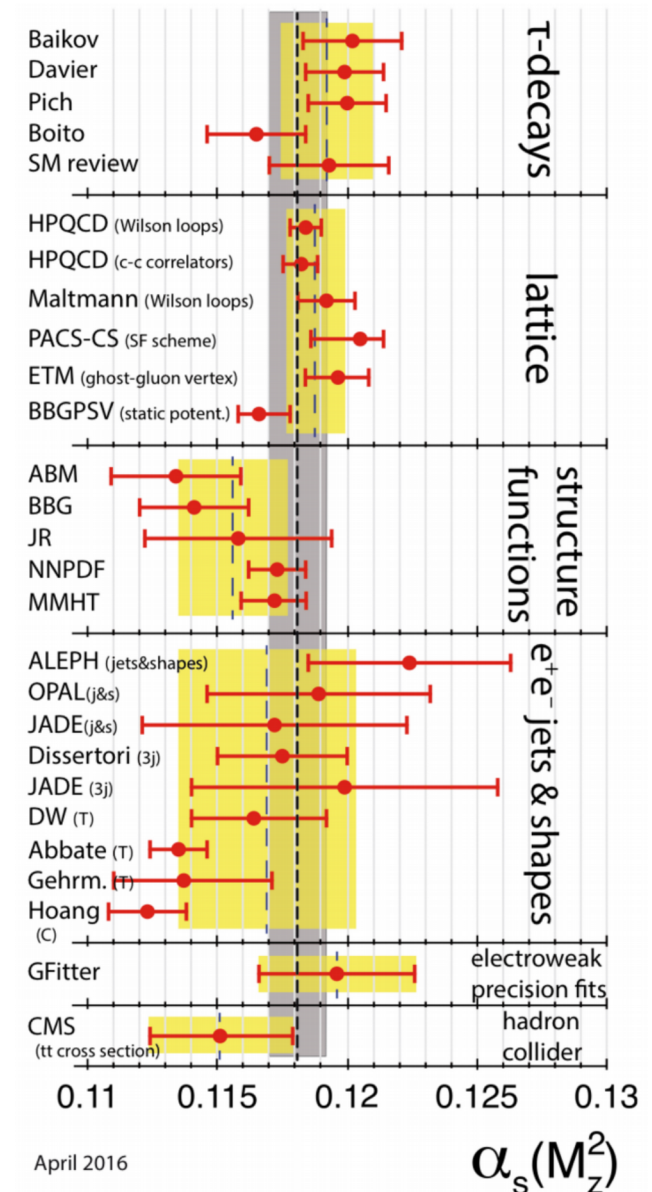
Parameter	Fit result	Correlation coefficients												
		$\alpha_s(m_Z)$	g_B	g_C	g_D	\tilde{u}_B	\tilde{u}_C	\tilde{u}_E	\tilde{d}_B	\tilde{d}_C	\bar{U}_C	\bar{D}_A	\bar{D}_B	\bar{D}_C
$\alpha_s(m_Z)$	0.1142 ± 0.0011	1												
g_B	-0.023 ± 0.035	0.25	1											
g_C	5.69 ± 4.09	-0.08	0.01	1										
g_D	-0.44 ± 4.20	-0.03	-0.10	0.99	1									
\tilde{u}_B	0.707 ± 0.036	0.39	0.25	0.05	0.04	1								
\tilde{u}_C	4.909 ± 0.096	-0.09	-0.13	0.02	0.03	-0.08	1							
\tilde{u}_E	12.7 ± 1.8	-0.03	-0.25	-0.04	-0.01	-0.75	0.57	1						
\tilde{d}_B	1.036 ± 0.098	0.24	-0.02	0.06	0.08	0.32	-0.24	-0.24	1					
\tilde{d}_C	5.35 ± 0.49	-0.10	-0.07	0.03	0.05	-0.08	-0.24	0.00	0.80	1				
\bar{U}_C	4.96 ± 0.86	0.32	-0.28	-0.01	0.05	0.76	0.09	-0.39	0.53	0.11	1			
\bar{D}_A	0.299 ± 0.032	0.29	-0.71	-0.04	0.07	0.32	0.01	-0.08	0.38	0.13	0.71	1		
\bar{D}_B	-0.091 ± 0.017	0.22	-0.79	-0.05	0.06	0.19	0.03	0.01	0.29	0.09	0.61	0.97	1	
\bar{D}_C	16.1 ± 3.8	-0.13	-0.51	-0.01	0.08	-0.15	-0.24	-0.06	0.14	0.24	0.05	0.48	0.46	1
g_A	2.84	constrained by sum-rules												
\tilde{u}_A	4.11	constrained by sum-rules												
\tilde{d}_A	6.94	constrained by sum-rules												
\bar{U}_A	1.80	set equal to $\bar{D}_A(1 - f_s)$												
\bar{U}_B	-0.091	set equal to \bar{D}_B												

History of Alpha Strong

- The current world average value $\alpha_s(m_Z) = 0.1181(11)$
- Mostly driven by lattice and tau-decays
- From LHC the most precise estimate is from $t\bar{t}$ (NNLO)



At least NNLO fits [PDG16]



April 2016

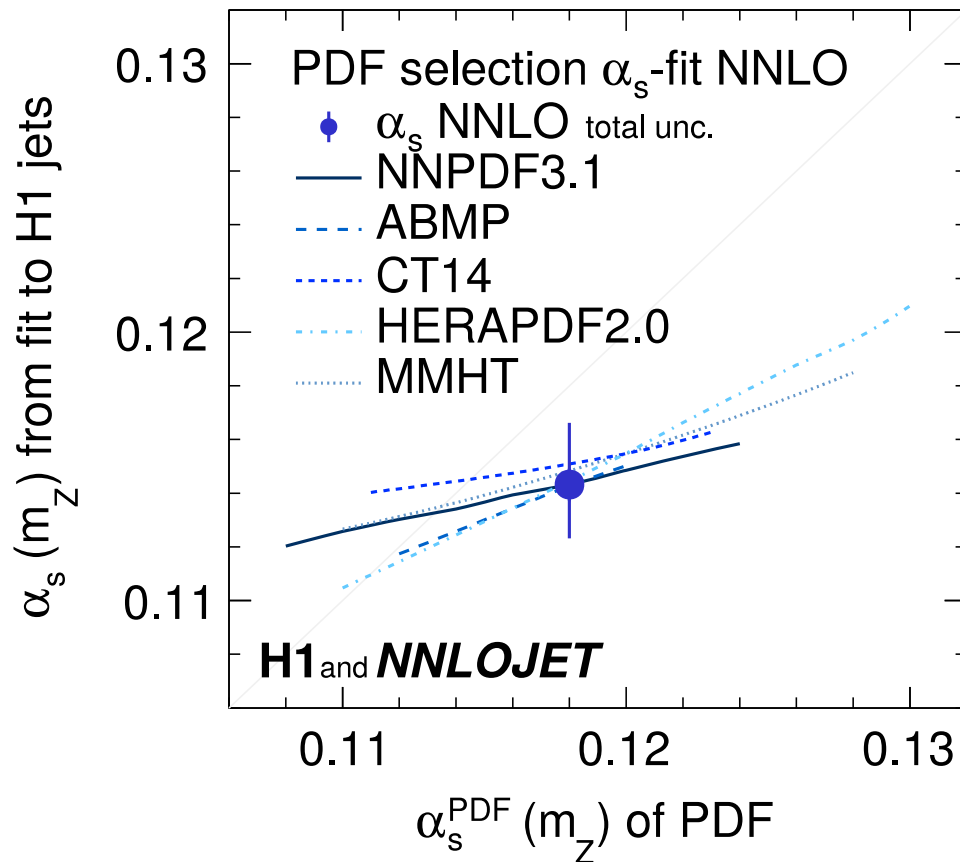
$\alpha_s(M_Z^2)$ 36

Dependence on PDF and α_S^{PDF}

In full H1 jet data sample
positive correlation
between α_S^{PDF} and α_S

Restricting to $\tilde{\mu} > 28 \text{ GeV}$
makes the α_S -fit
uncorrelated to α_S^{PDF}

H1 jets



H1 jets ($\tilde{\mu} > 28 \text{ GeV}$)

